A Resilience-Oriented Multi-Stage Adaptive Distribution System Planning Considering Multiple Extreme Weather Events

Siyuan Wang, *Member, IEEE*, Rui Bo, *Senior Member, IEEE*

***Abstract*—Climate change may increase the risk of an area being hit by multiple extreme weather events, which brings significant challenges for distribution system planners in an increasing renewable penetration era. There is an urgent need for planning approaches to be more flexible and allow for adaptive adjustments in the future to hedge against high uncertainties in extreme weather event scenarios. In this work, we propose a resilience-oriented distribution system planning approach that considers multiple extreme weather events. A multi-stage hybrid-stochastic-and-robust formulation is developed to model decisions not only for initial investments, but also for adaptive investments and emergent operations in response to particular extreme events, meanwhile considering both long-term and short-term uncertainties. Our model is solved by a novel progressive hedging algorithm that is embedded with a nested column-and-constraint generation method. Case studies demonstrate the benefits of the proposed approach in making flexible and affordable planning decisions to protect distribution systems against multiple extreme weather events.**

***Index Terms*—resilience-oriented planning, distribution system resilience, multi-stage adaptive optimization, multiple extreme weather events, mobile energy storage.**

NOMENCLATURE

Notations used in sections II-A to II-C are defined here. For the sake of simplicity, notations used in abstract formulation and algorithm are explained in sections II-D and III.

Indices and Sets

s, t	Indices for scenarios and time periods.
b, m, n	Indices for buses. m and n are used to represent terminal buses of distribution line (m, n).
i	Index for renewable energy resources, loads, and mobile storage units.
$\mathcal{S}, \mathcal{T}, \mathcal{B}$	Sets of scenarios, time periods, and buses.
$\mathcal{B}^{\text{root}}, \mathcal{B}_i^{\text{mes}}$	Sets of root bus(es), and buses that are portable for mobile storage i.
$\mathcal{S}^{\text{nml}}, \mathcal{S}^{\text{xtm}}$	Sets of normal and extreme weather scenarios, i.e., $\mathcal{S} = \mathcal{S}^{\text{nml}} \cup \mathcal{S}^{\text{xtm}}$.
$\mathcal{L}, \mathcal{L}^{\text{tie}}$	Sets of existing regular lines and tie-lines.
$\mathcal{L}^{\text{new}}$	Set of candidate regular lines.
$\mathcal{L}_s^{\text{har}}$	Set of candidate lines to harden.
Ω^{circles}	Set of all circles in the undirected graph that represents bus-line relations of a system.
$\mathcal{L}_k^{\text{circle}}$	Set of branches in circle $k \in \Omega^{\text{circles}}$.
$\mathcal{E}^{\text{new}}$	Set of candidate mobile storage.
$\mathcal{W}, \mathcal{W}^{\text{new}}$	Sets of existing and candidate renewable energy resources.
$\mathcal{D}$	Set of loads.
$\cdot_b$	Set of devices $\cdot$ connected to bus b.

Parameters

Pr_s	Probability of scenario s.
n^{d}	Number of days in a year.
$c_i^{\text{inv}}, c_{m,n}^{\text{inv}}$	Annualized investment costs of candidate renewable energy resource i and line (m, n).
$\overline{P}_i^{\max}$	Maximum power capacity for candidate renewable energy resource or mobile storage i.
$\overline{E}_i^{\max}$	Maximum energy capacity for candidate mobile storage i.
$c_{i,s}^{\text{pcap}}, c_{i,s}^{\text{ecap}}$	Re-investment costs per unit power capacity and per unit energy capacity for renting candidate mobile storage i in scenario s.
$c_{m,n,s}^{\text{har}}$	Re-investment cost for hardening line (m, n) in scenario s.
$n_s^{\max}$	Maximum number of hardened lines in scenario s.
$\text{Pr}_{m,n,s,t}^{\text{line}}$	Probability of line outage in time period t if line (m, n) is not hardened.
$\text{Pr}_{i,s,t}^{\text{res}}$	Probability of renewable energy resource i outage in time period t.
$\text{T}_{m,n}^{\text{repair}}$	Repair time for an outage of line (m, n).
$\text{T}_i^{\text{repair}}$	Repair time for an outage of renewable energy resources i.
W	Uncertainty budget for outages.
c_i^{LOL}	Penalty for loss of load i.
$c_i^{\text{ch}}, c_i^{\text{dc}}$	Charging and discharging operation costs for mobile storage i.
$\hat{\lambda}_{b,s,t}$	Local marginal price (LMP) at root bus b.
$p_{i,s,t}^{\text{D}}, q_{i,s,t}^{\text{D}}$	Active and reactive power of load i.
$\overline{\rho}_{i,s,t}$	Shedding ratio limit for load i.
$\overline{V}_b, \underline{V}_b$	Upper and lower bounds for voltage at bus b.
$\text{LOL}_s^{\max}$	Maximum loss of load in scenario s.
$r_{m,n}, x_{m,n}$	Resistance and reactance of line (m, n).
$\text{M}_{m,n}$	Big-M value for constraints related to distribution line (m, n).
$S_{m,n}$	Rating of distribution line (m, n).

Paper no. TSTE-00225-2022. (*Corresponding author: Rui Bo.*)

Siyuan Wang was with the Department of Electrical and Computer Engineering, Missouri University of Science and Technology, MO 65409 USA, where he worked on this paper. He is now with the Whiting School of Engineering, Johns Hopkins University, Baltimore, MD 21218, USA (e-mail: siyuanwang@mst.edu; siyuanwang@jhu.edu).

Rui Bo is with the Department of Electrical and Computer Engineering, Missouri University of Science and Technology, MO 65409 USA (e-mail: rbo@mst.edu).

This article has been accepted for publication in IEEE Transactions on Sustainable Energy. DOI: 10.1109/TSTE.2023.3234916.
© 2023 IEEE. Personal use of this material is permitted. Permission from IEEE must be obtained for all other uses, in any current or future media, including reprinting/republishing this material for advertising or promotional purposes, creating new collective works, for resale or redistribution to servers or lists, or reuse of any copyrighted component of this work in other works.

n^{LA} Number of linear constraints to approximate a line rating constraint.

$\phi^k_{m,n}, \chi^k_{m,n}, \psi^k_{m,n}$ Parameters in the k-th linear approximated rating constraint for line (m,n).

$\hat{p}^{\max}_i$ Capacity of existing renewable energy resource i.

$w^{\mathrm{res}}_{i,s,t}$ Normalized available capacity of existing and candidate renewable energy resource i.

$\overline{d}^{\mathrm{mes}}_i, \underline{d}^{\mathrm{mes}}_i$ Upper and lower bounds for the duration of mobile storage i.

$\eta^{\mathrm{ch}}_i, \eta^{\mathrm{dc}}_i$ Charging and discharging efficiencies of mobile storage i.

$\gamma_{i,0}, \underline{\gamma}_i$ Normalized initial state of charge (SOC) and SOC lower bound for mobile storage i.

Decision Variables in Uncertainty Sets

$o^{\mathrm{line}}_{m,n,s,t}, v^{\mathrm{line}}_{m,n,s,t}$ Binary variables indicating whether line (m,n) is supposed to be in an outage and start an outage in time period t of scenarios s if it is not hardened.

$o^{\mathrm{res}}_{i,s,t}, v^{\mathrm{res}}_{i,s,t}$ Binary variables indicating whether renewable energy resource i is in an outage and starts an outage in time period t of scenarios s.

Decision Variables

$z^{\mathrm{cons}}_{m,n}$ Binary variables indicating whether constructing candidate line (m,n).

$p^{\max}_i$ Capacity of candidate renewable energy resource i.

$z^{\mathrm{har}}_{m,n,s}$ Binary variables indicating whether hardening candidate line (m,n) for extreme scenario s.

$z^{\mathrm{on}}_{m,n,s,t}$ Binary variables indicating whether the switch of tie-line (m,n) is on in time period t of scenarios s.

$u^{\mathrm{line}}_{m,n,s,t}$ Variables indicating connection status of line (m,n) in time period t of scenarios s.

$p^{\max}_{i,s}, e^{\max}_{i,s}$ Power and energy capacities of candidate mobile storage i for extreme scenario s.

$p^{\mathrm{root}}_{b,s,t}, q^{\mathrm{root}}_{b,s,t}$ Active and reactive power from the bulk power system through root bus b in time period t.

$f^{\mathrm{P}}_{m,n,s,t}, f^{\mathrm{Q}}_{m,n,s,t}$ Active and reactive power flow in line (m,n) in time period t.

$u_{b,s,t}$ Squared voltage magnitude of bus b in time period t. Using $v_{b,s,t}$ to represent voltage magnitude, we have $u_{b,s,t} = v^2_{b,s,t}$.

$\rho_{i,s,t}$ Shedding ratio for load i in time period t.

$p_{i,s,t}, q_{i,s,t}$ Active and reactive power from renewable energy resource i in time period t. Reactive power from mobile storage i is also denoted by $q_{i,s,t}$.

$\alpha_{i,b,s,t}$ Binary variables indicating connection status of mobile storage i to bus b in time period t.

$p_{i,b,s,t}, q_{i,b,s,t}$ Active and reactive power from mobile storage i injected to bus b in time period t.

$e_{i,s,t}$ SOC of mobile storage i in time period t.

$\beta^{\mathrm{ch}}_{i,s,t}, \beta^{\mathrm{dc}}_{i,s,t}$ Binary variables indicating whether mobile storage i is in the charging or discharging mode in time period t.

$p^{\mathrm{ch}}_{i,s,t}, p^{\mathrm{dc}}_{i,s,t}$ Active charging and discharging power of mobile storage i in time period t.

I. Introduction

EXTREME weather events have frequently been happening all over the world, which threatens the secure operations of power distribution grids, especially for those with renewable energy resources. A notable trend is an increasing occurrence of being hit by more than one extreme weather event in one specific area. A well-known example is Texas, which has suffered from power outages or received outage warnings due to heat waves [1], [2], hurricanes [3], and the unusual February 2021 winter storm [4]. Multiple disastrous events in one area have also been identified in other countries, such as India [5] and Australia [6].

Although multiple extreme events may not usually come at once, distribution system planners need to consider them all from a planning perspective. In addition, we may not assume specific extreme weather events would not happen based on their rare historical occurrences, which is a lesson learned from the Texas winter storm in February 2021. However, if planners consider various events unlikely to happen in system planning, the resultant decisions might be over-conservative and unaffordable. Therefore, planning approaches are expected to be flexible for adaptive adjustments in the future to hedge against uncertainties in extreme weather event scenarios. To address increasing uncertainties that may appear in future power systems, the adaptive adjustment capability of flexible generation resources depending on the partial realization of uncertainties has been leveraged for day-ahead unit commitment [7]–[9]. In the context of bulk power system planning, the work in [10] shows how flexible planning decisions can adapt to future high-impact uncertainties at reasonable costs when considering a multi-stage decision-making process in a long horizon. In terms of distribution systems, there is an urgent need for flexible adaptive planning approaches that can affordably address high uncertainties in the happening of multiple extreme events.

After early warnings are received, re-investments in mobile storage facilities and distribution line hardening provide flexible planning options for resilience enhancement. *On the mobile storage side*, authors of [11] propose a two-stage dispatch framework that considers pre-positioning and real-time allocation for truck-mounted mobile emergency generators, which includes mobile storage, in response to natural disasters. Repair crew dispatch is further incorporated in [12] to co-optimize with mobile storage for a resilient disaster recovery. In [13], the roles of various types of PV systems are considered in a two-stage stochastic pre-event preparation model. These works address the pre-positioning, real-time allocation, and post-disaster recovery topics in distribution system operations. From a planning perspective, authors of [14] propose a two-stage stochastic mobile storage investment model that considers routing decisions in the second stage to enhance the distribution system resilience. *On the distribution line hardening side*, an optimal hardening strategy is proposed in [15] to protect lines against extreme weather events, in which

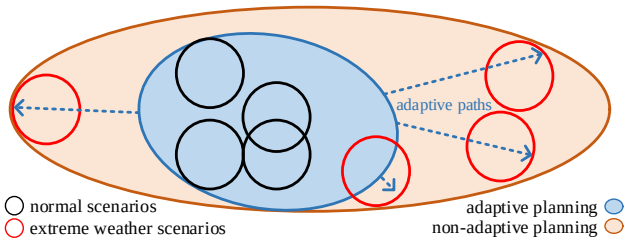

Fig. 1. Illustration of adaptive planning.

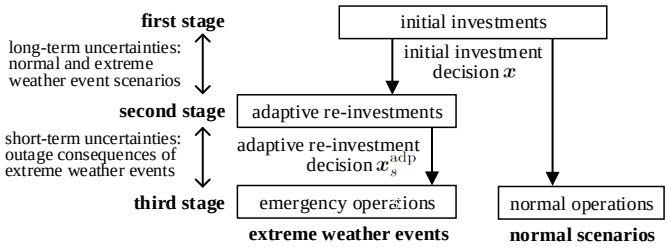

Fig. 2. Modeling framework ($\boldsymbol{x}$ and $\boldsymbol{x}_s^{\mathrm{adp}}$ are defined in section II).

a min-max-min optimization model is developed. In [16], hardening decisions are made in a two-stage mixed-integer program model considering both during-event operation cost and after-event repair cost. In [17], network reconfiguration and islanding are further incorporated in a two-stage robust hardening model.

These works provide valuable insights into flexible planning options for distribution systems usually in the context of two-stage stochastic programming or robust optimization. They rarely consider both mobile storage renting and distribution line hardening in a framework wherein adaptive planning flexibility can be leveraged to handle possible happenings of multiple extreme weather events. It is worth mentioning that the works in [18] and [19] incorporate line hardening and backup generator allocation, while not considering mobile storage. In these two works, two-stage optimization models are formulated assuming event-preparation planning decisions are independent of extreme scenarios. To make better use of the aforementioned flexible adaptive planning options, we propose a novel multi-stage hybrid-stochastic-and-robust model that considers both long-term uncertainties in extreme weather event scenarios, and short-term uncertainties in outage consequences when specific extreme events happen. Adaptive stochastic modeling is adopted to handle high long-term uncertainties, which allows making initial and flexible adaptive investments for possible happenings of multiple extreme weather events. As illustrated in Fig. 1, this can enable reduced conservativeness and therefore improved affordability of the initial investment decisions. For extreme events, a robust mechanism is used to represent resilient short-term uncertainty management after early warnings are received.

On the other hand, solving the proposed multi-stage hybrid-stochastic-and-robust model is challenging. Progressive hedging (PH) is a traditional method to solve stochastic optimization problems [20], which can also be used as an effective heuristic for optimizations with discrete decision variables [21]. However, PH cannot be directly applied to our hybrid-stochastic-and-robust model. To address this need, we propose a novel PH algorithm that is embedded with a nested column-and-constraint generation (CCG) procedure. The nested CCG approach originally proposed in [22] is capable of iteratively identifying worst-case short-term uncertainty realizations, and converting our problem to a stochastic formulation with identified realizations. Consequently, the revised PH method can be used to solve the whole model in our proposed approach.

The main contributions of this work are:

- We propose a resilience-oriented distribution system planning approach that can represent flexible adaptive investments. Our numerical experiments show that flexible adaptive investments can reduce the conservativeness of planning decisions when multiple low-probability extreme weather events are simultaneously considered.
- We formulate a multi-stage hybrid-stochastic-and-robust model that takes both long-term and short-term uncertainties into account. To address the computational challenges in solving the proposed model, we develop a novel PH algorithm that is embedded with a nested CCG procedure.

II. Multi-Stage Resilience-Oriented Adaptive Planning Model

The proposed resilience-oriented planning, as shown in Fig. 2, considers decisions made in three stages: The *first stage* makes here-and-now decisions for initial planning, which includes investments for renewable energy resources and distribution lines; the *second stage* decides adaptive re-investments on urgent mobile storage renting and distribution line hardening, in response to specific extreme events when early warnings are received; the *third stage* models normal scenarios to represent daily system operations, and emergent scenarios to reduce the impact of extreme events.

A. First Stage: Initial Investments

The decisions for renewable energy resource and distribution line co-investments are made in the first-stage problem in (1). The objective function shown in (1a) includes the initial investment cost and the expected cost for future stages. By denoting first-stage decision variables by $\boldsymbol{x}$, we use $\varphi_s(\boldsymbol{x})$ and $\vartheta_s(\boldsymbol{x})$ to present daily costs for extreme weather events and normal conditions, which are defined later in this section. Capacities of candidate renewable energy resources are bounded in (1b). Binary variables for distribution line investments are declared in (1c).

$$\min_{\boldsymbol{x}} \quad \sum_{i\in\mathcal{W}^{\mathrm{new}}} c_i^{\mathrm{inv}} p_i^{\max} + \sum_{(m,n)\in\mathcal{L}^{\mathrm{new}}} c_{m,n}^{\mathrm{inv}} z_{m,n}^{\mathrm{cons}} + \left(\sum_{s\in\mathcal{S}^{\mathrm{xtm}}} \Pr_s \cdot \varphi_s(\boldsymbol{x}) + \sum_{s\in\mathcal{S}^{\mathrm{nml}}} \Pr_s \cdot \vartheta_s(\boldsymbol{x}) \right) \cdot n^{\mathrm{d}} \tag{1a}$$

$$\text{s.t.} \quad 0 \le p_i^{\max} \le \overline{P}_i^{\max}, \ \forall i \in \mathcal{W}^{\mathrm{new}} \tag{1b}$$

$$z_{m,n}^{\mathrm{cons}} \in \{0,1\}, \ \forall (m,n) \in \mathcal{L}^{\mathrm{new}} \tag{1c}$$

where, $\boldsymbol{x} = \{z_{m,n}^{\mathrm{cons}}, \forall (m,n) \in \mathcal{L}^{\mathrm{new}};\ p_i^{\max}, \forall i \in \mathcal{W}^{\mathrm{new}}\}$.

B. Second Stage: Re-Investments for Extreme Weather Events

Renting mobile storage and hardening distribution lines are considered emergent re-investment approaches to prepare for extreme weather events. For each such event $s \in \mathcal{S}^{\mathrm{xtm}}$, the objective function $\varphi_s(\boldsymbol{x})$ calculates re-investment cost and future operation cost. In (2a), $\vartheta_s(\boldsymbol{x}, \boldsymbol{x}_s^{\mathrm{adp}}, \hat{\boldsymbol{u}}_s)$ and $\tilde{\vartheta}_s(\boldsymbol{x}, \boldsymbol{x}_s^{\mathrm{adp}}, \boldsymbol{u}_s)$ are the operation cost under the base case and big-M penalty for infeasibility under the worst case, as further defined in (4) and (16), respectively. Vectors $\boldsymbol{x}_s^{\mathrm{adp}}$ and $\boldsymbol{u}_s$ represent second-stage re-investment decision variables and event consequence variables, respectively; $\hat{\boldsymbol{u}}_s$ denotes event consequence variables $\boldsymbol{u}_s$ in the base case. The power and energy capacities of mobile storage are bounded in (2b) and (2c), respectively. The line hardening decision is dependent on the construction decision, as indicated in (2d). The number of lines that can be emergently hardened is limited by the availability of crew and time, as modeled in (2e). Binary hardening decision variables are declared in (2f).

$$\begin{aligned}\varphi_s(\boldsymbol{x}) = &\min_{\boldsymbol{x}_s^{\mathrm{adp}}} \sum_{i\in\mathcal{E}^{\mathrm{new}}} \left(c_{i,s}^{\mathrm{pcap}} p_{i,s}^{\max} + c_{i,s}^{\mathrm{ecap}} e_{i,s}^{\max}\right) \\ &+ \sum_{(m,n)\in\mathcal{L}_s^{\mathrm{har}}} c_{m,n,s}^{\mathrm{har}} z_{m,n,s}^{\mathrm{har}} + \vartheta_s(\boldsymbol{x}, \boldsymbol{x}_s^{\mathrm{adp}}, \hat{\boldsymbol{u}}_s) \\ &+ \max_{\boldsymbol{u}_s\in\mathcal{U}_s^{\mathrm{xtm}}} \tilde{\vartheta}_s(\boldsymbol{x}, \boldsymbol{x}_s^{\mathrm{adp}}, \boldsymbol{u}_s) \qquad (2a)\end{aligned}$$

$$\text{s.t.} \quad 0 \le p_{i,s}^{\max} \le \overline{P}_i^{\max},\ \forall i \in \mathcal{E}^{\mathrm{new}} \qquad (2b)$$

$$\underline{d}_i^{\mathrm{mes}} p_{i,s}^{\max} \le e_{i,s}^{\max} \le \overline{d}_i^{\mathrm{mes}} p_{i,s}^{\max},\ e_{i,s}^{\max} \le \overline{E}_i^{\max}, \quad \forall i \in \mathcal{E}^{\mathrm{new}} \qquad (2c)$$

$$z_{m,n,s}^{\mathrm{har}} \le z_{m,n}^{\mathrm{cons}},\ \forall (m,n) \in \mathcal{L}^{\mathrm{new}} \cap \mathcal{L}_s^{\mathrm{har}} \qquad (2d)$$

$$\sum_{(m,n)\in\mathcal{L}_s^{\mathrm{har}}} z_{m,n,s}^{\mathrm{har}} \le n_s^{\max} \qquad (2e)$$

$$z_{m,n,s}^{\mathrm{har}} \in \{0,1\},\ \forall (m,n) \in \mathcal{L}_s^{\mathrm{har}} \qquad (2f)$$

where, $\boldsymbol{x}_s^{\mathrm{adp}} = \{z_{m,n,s}^{\mathrm{har}}, \forall (m,n) \in \mathcal{L}_s^{\mathrm{har}};\ p_{i,s}^{\max}, e_{i,s}^{\max}, \forall i \in \mathcal{E}^{\mathrm{new}}\}$, and $\boldsymbol{u}_s = \{o_{m,n,s,t}^{\mathrm{line}}, \forall (m,n) \in \mathcal{L} \cup \mathcal{L}^{\mathrm{new}} \cup \mathcal{L}^{\mathrm{tie}}, \forall t \in \mathcal{T};\ o_{i,s,t}^{\mathrm{res}}, \forall i \in \mathcal{W} \cup \mathcal{W}^{\mathrm{new}}, \forall t \in \mathcal{T}\}$.

The uncertainty set $\mathcal{U}_s^{\mathrm{xtm}}$ for outage consequences on distribution lines and renewable energy resources is constructed in (3). In (3a), the uncertainty budget W for each time period is defined based on Claude Shannon's concept of information [15], [23]. Here outages are considered to be mutually independent. Note variables $o_{m,n,s,t}^{\mathrm{line}}$ indicate outage statuses if line (m,n) is not hardened. In (3b) and (3c), the relations between outage-starting indicator variables and outage status variables are constructed considering repair time. Outage events are assumed to happen at most once for each device in a daily scenario, as modeled in (3d) and (3e). Binary variables are declared in (3f). Outages of mobile energy storage units are not considered, as they can be kept in safe places when extreme events happen.

$$\begin{aligned}\mathcal{U}_s^{\mathrm{xtm}} = \Bigg\{ &o_{m,n,s,t}^{\mathrm{line}}, \forall (m,n) \in \mathcal{L} \cup \mathcal{L}^{\mathrm{new}} \cup \mathcal{L}^{\mathrm{tie}}, \forall t \in \mathcal{T}; \\ &o_{i,s,t}^{\mathrm{res}}, \forall i \in \mathcal{W} \cup \mathcal{W}^{\mathrm{new}}, \forall t \in \mathcal{T}: \\ &\sum_{(m,n)\in\mathcal{L}\cup\mathcal{L}^{\mathrm{new}}\cup\mathcal{L}^{\mathrm{tie}}} \left(-\log_2 \Pr_{m,n,s,t}^{\mathrm{line}}\right) \cdot v_{m,n,s,t}^{\mathrm{line}} \\ &+ \sum_{i\in\mathcal{W}\cup\mathcal{W}^{\mathrm{new}}} \left(-\log_2 \Pr_{i,s,t}^{\mathrm{res}}\right) \cdot v_{i,s,t}^{\mathrm{res}} \le W,\ \forall t \in \mathcal{T} \qquad (3a)\end{aligned}$$

$$o_{m,n,s,t}^{\mathrm{line}} = \sum_{t'=t-\mathrm{T}_{m,n}^{\mathrm{repair}}+1}^{t} v_{m,n,s,t'}^{\mathrm{line}}, \quad \forall (m,n) \in \mathcal{L} \cup \mathcal{L}^{\mathrm{new}} \cup \mathcal{L}^{\mathrm{tie}}, \forall t \in \mathcal{T} \qquad (3b)$$

$$o_{i,s,t}^{\mathrm{res}} = \sum_{t'=t-\mathrm{T}_{i}^{\mathrm{repair}}+1}^{t} v_{i,s,t'}^{\mathrm{res}},\ \forall i \in \mathcal{W} \cup \mathcal{W}^{\mathrm{new}}, \forall t \in \mathcal{T} \qquad (3c)$$

$$\sum_{t'\in\mathcal{T}} v_{m,n,s,t'}^{\mathrm{line}} \le 1,\ \forall (m,n) \in \mathcal{L} \cup \mathcal{L}^{\mathrm{new}} \cup \mathcal{L}^{\mathrm{tie}} \qquad (3d)$$

$$\sum_{t'\in\mathcal{T}} v_{i,s,t'}^{\mathrm{res}} \le 1,\ \forall i \in \mathcal{W} \cup \mathcal{W}^{\mathrm{new}} \qquad (3e)$$

$$\begin{aligned}&o_{m,n,s,t}^{\mathrm{line}}, o_{i,s,t}^{\mathrm{res}}, v_{m,n,s,t}^{\mathrm{line}}, v_{i,s,t}^{\mathrm{res}} \in \{0,1\}, \\ &\forall (m,n) \in \mathcal{L} \cup \mathcal{L}^{\mathrm{new}} \cup \mathcal{L}^{\mathrm{tie}}, \forall i \in \mathcal{W} \cup \mathcal{W}^{\mathrm{new}}, \forall t \in \mathcal{T}\Bigg\} \qquad (3f)\end{aligned}$$

For normal scenarios $s \in \mathcal{S}^{\mathrm{nml}}$, this stage is not modeled because usually no re-investment decisions need to be made.

C. Third Stage: System Operations

The distribution system operations are formulated in the third stage. We first present a model for extreme weather event scenarios $s \in \mathcal{S}^{\mathrm{xtm}}$, which can be simplified for normal scenarios $s \in \mathcal{S}^{\mathrm{nml}}$.

1) Objective Function: The third-stage problem aims to minimize the system operation cost, which is the sum of load shedding cost, mobile storage operation cost, and power purchasing cost from the bulk power system.

$$\begin{aligned}\vartheta_s(\boldsymbol{x}, \boldsymbol{x}_s^{\mathrm{adp}}, \boldsymbol{u}_s) = \min_{\boldsymbol{y}_s} \sum_{t\in\mathcal{T}} \Bigg\{ &\sum_{b\in\mathcal{B}^{\mathrm{root}}} \hat{\lambda}_{b,s,t} p_{b,s,t}^{\mathrm{root}} + \\ &\sum_{i\in\mathcal{D}} c_i^{\mathrm{LOL}} \rho_{i,s,t} p_{i,s,t}^{\mathrm{D}} + \sum_{\forall i\in\mathcal{E}^{\mathrm{new}}} \left(c_i^{\mathrm{dc}} p_{i,s,t}^{\mathrm{dc}} + c_i^{\mathrm{ch}} p_{i,s,t}^{\mathrm{ch}}\right) \Bigg\} \qquad (4)\end{aligned}$$

where, operation decision variables $\boldsymbol{y}_s = \{u_{b,s,t},\ \forall b \in \mathcal{B}, \forall t \in \mathcal{T};\ p_{b,s,t}^{\mathrm{root}},\ q_{b,s,t}^{\mathrm{root}},\ \forall b \in \mathcal{B}^{\mathrm{root}},\ \forall t \in \mathcal{T};\ \rho_{i,s,t},\ \forall i \in \mathcal{D}, \forall t \in \mathcal{T};\ u_{m,n,s,t}^{\mathrm{line}},\ \forall (m,\ n) \in \mathcal{L} \cup \mathcal{L}^{\mathrm{new}} \cup \mathcal{L}^{\mathrm{tie}},\ \forall t \in \mathcal{T};\ z_{m,n,s,t}^{\mathrm{on}},\ \forall (m,\ n) \in \mathcal{L}^{\mathrm{tie}},\ \forall t \in \mathcal{T};\ f_{m,n,s,t}^{\mathrm{P}},\ f_{m,n,s,t}^{\mathrm{Q}},\ \forall (m, n) \in \mathcal{L} \cup \mathcal{L}^{\mathrm{new}} \cup \mathcal{L}^{\mathrm{tie}}, \forall t \in \mathcal{T};\ p_{i,s,t}, q_{i,s,t}, \forall i \in \mathcal{W} \cup \mathcal{W}^{\mathrm{new}}, \forall t \in \mathcal{T};\ p_{i,s,t}^{\mathrm{dc}},\ p_{i,s,t}^{\mathrm{ch}},\ q_{i,s,t},\ \beta_{i,s,t}^{\mathrm{dc}},\ \beta_{i,s,t}^{\mathrm{ch}},\ e_{i,s,t},\ \forall i \in \mathcal{E}^{\mathrm{new}}, \forall t \in \mathcal{T};\ p_{i,b,s,t}, q_{i,b,s,t}, \alpha_{i,b,s,t}, \forall i \in \mathcal{E}^{\mathrm{new}}, \forall b \in \mathcal{B}, \forall t \in \mathcal{T}\}$.

2) Nodal Constraints: Nodal active and reactive power balance constraints are presented in (5a) and (5b), respectively. The voltage magnitude is bounded in (5c), in which a square form is used to be compatible with the formulation in (7).

$$\begin{aligned}&\sum_{(b,n)\in\mathcal{L}\cup\mathcal{L}^{\mathrm{new}}\cup\mathcal{L}^{\mathrm{tie}}} f_{b,n,s,t}^{\mathrm{P}} - \sum_{(m,b)\in\mathcal{L}\cup\mathcal{L}^{\mathrm{new}}\cup\mathcal{L}^{\mathrm{tie}}} f_{m,b,s,t}^{\mathrm{P}} = \\ &\sum_{b'\in\mathcal{B}^{\mathrm{root}}\cap\{b\}} p_{b',s,t}^{\mathrm{root}} + \sum_{i\in\mathcal{E}^{\mathrm{new}}, b'\in\mathcal{B}_i^{\mathrm{mes}}\cap\{b\}} p_{i,b',s,t} \\ &+ \sum_{i\in\mathcal{W}_b\cup\mathcal{W}_b^{\mathrm{new}}} p_{i,s,t} - \sum_{i\in\mathcal{D}_b} (1-\rho_{i,s,t}) \cdot p_{i,s,t}^{\mathrm{D}}, \\ &\qquad \forall b \in \mathcal{B}, \forall t \in \mathcal{T} \qquad (5a)\end{aligned}$$

$$\sum_{(b,n)\in\mathcal{L}\cup\mathcal{L}^{\mathrm{new}}\cup\mathcal{L}^{\mathrm{tie}}} f_{b,n,s,t}^{\mathrm{Q}} - \sum_{(m,b)\in\mathcal{L}\cup\mathcal{L}^{\mathrm{new}}\cup\mathcal{L}^{\mathrm{tie}}} f_{m,b,s,t}^{\mathrm{Q}} =$$

$$\sum_{b'\in\mathcal{B}^{\text{root}}\cap\{b\}} q^{\text{root}}_{b',s,t} + \sum_{i\in\mathcal{E}^{\text{new}},b'\in\mathcal{B}^{\text{mes}}_i\cap\{b\}} q_{i,b',s,t} + \sum_{i\in\mathcal{W}_b\cup\mathcal{W}^{\text{new}}_b} q_{i,s,t} - \sum_{i\in\mathcal{D}_b}(1-\rho_{i,s,t})\cdot q^{\text{D}}_{i,s,t}, \quad \forall b\in\mathcal{B},\forall t\in\mathcal{T} \tag{5b}$$

$$\underline{V}_b^2 \le u_{b,s,t} \le \overline{V}_b^2,\ \forall b\in\mathcal{B},\forall t\in\mathcal{T} \tag{5c}$$

3) Load Constraints: The shedding ratio $\rho_{i,s,t}$ is bounded for each load i in (6a). Specially, $\overline{\rho}_{i,s,t}=0$ for critical loads. From a system perspective, the total loss of load in scenario s is expected to be limited by $\text{LOL}^{\max}_s$ in (6b) with proper planning decisions.

$$0\le\rho_{i,s,t}\le\overline{\rho}_{i,s,t},\ \forall i\in\mathcal{D},\forall t\in\mathcal{T} \tag{6a}$$

$$\sum_{i\in\mathcal{D}}\sum_{t\in\mathcal{T}}\rho_{i,s,t}\cdot p^{\text{D}}_{i,s,t}\le\text{LOL}^{\max}_s \tag{6b}$$

4) Distribution Line Constraints: Linear *DistFlow* equations [24] for distribution system power flow calculation are adopted in (7a)-(7b) with a big-M method to control the line connection statuses. Line flows are limited in (7c), which also ensures that active and reactive line flows are zero when a line is not connected. The radiality constraint of the distribution network is modeled in (7d), wherein Ω^{circles} is the set of all circles from a graph theory point of view and $\mathcal{L}^{\text{circle}}_k$ is the set of branches in circle k.

$$u_{m,s,t}-u_{n,s,t}-2\left(r_{m,n}\cdot f^{\text{P}}_{m,n,s,t}+x_{m,n}\cdot f^{\text{Q}}_{m,n,s,t}\right) \le \text{M}_{m,n}\cdot(1-u^{\text{line}}_{m,n,s,t}), \quad \forall(m,n)\in\mathcal{L}\cup\mathcal{L}^{\text{tie}}\cup\mathcal{L}^{\text{new}},\forall t\in\mathcal{T} \tag{7a}$$

$$u_{m,s,t}-u_{n,s,t}-2\left(r_{m,n}\cdot f^{\text{P}}_{m,n,s,t}+x_{m,n}\cdot f^{\text{Q}}_{m,n,s,t}\right) \ge -\text{M}_{m,n}\cdot(1-u^{\text{line}}_{m,n,s,t}), \quad \forall(m,n)\in\mathcal{L}\cup\mathcal{L}^{\text{tie}}\cup\mathcal{L}^{\text{new}},\forall t\in\mathcal{T} \tag{7b}$$

$$f^{\text{P}\ 2}_{m,n,s,t}+f^{\text{Q}\ 2}_{m,n,s,t}\le S^2_{m,n}\cdot u^{\text{line}}_{m,n,s,t}, \quad \forall(m,n)\in\mathcal{L}\cup\mathcal{L}^{\text{tie}}\cup\mathcal{L}^{\text{new}},\forall t\in\mathcal{T} \tag{7c}$$

$$\sum_{(m,n)\in\mathcal{L}^{\text{circle}}_k} u_{m,n,s,t}\le|\mathcal{L}^{\text{circle}}_k|-1,\ \forall k\in\Omega^{\text{circles}},\forall t\in\mathcal{T} \tag{7d}$$

A good choice of big-M value in (7a)-(7b) could be helpful for numerical performance. When a line is not connected, i.e. $u^{\text{line}}_{m,n,s,t}=0$, we have $f^{\text{P}}_{m,n,s,t}=0$ and $f^{\text{Q}}_{m,n,s,t}=0$ from (7c). Therefore, in (7a) and (7b), $|u_{m,s,t}-u_{n,s,t}|$ is bounded by $\text{M}_{m,n}$. Big-M value $\text{M}_{m,n}$ is set as $(\overline{V}_m+\overline{V}_n)\cdot\max\{|\overline{V}_m-\underline{V}_n|,|\overline{V}_n-\underline{V}_m|\}$ for line (m,n), based on the bound derivation in (8).

$$\begin{aligned}|u_{m,s,t}-u_{n,s,t}| &= \left|v^2_{m,s,t}-v^2_{n,s,t}\right| \\ &= (v_{m,s,t}+v_{n,s,t})\left|v_{m,s,t}-v_{n,s,t}\right| \\ &\le \left(\overline{V}_m+\overline{V}_n\right)\cdot\max\left\{\left|\overline{V}_m-\underline{V}_n\right|,\left|\overline{V}_n-\underline{V}_m\right|\right\}\end{aligned} \tag{8}$$

Flow limit constraints in (7c) are further linearized in (9) with n^{LA} mixed-integer linear constraints [25].

$$\phi^k_{m,n}f^{\text{P}}_{m,n,s,t}+\chi^k_{m,n}f^{\text{Q}}_{m,n,s,t}\le\psi^k_{m,n}u^{\text{line}}_{m,n,s,t}, \quad \forall(m,n)\in\mathcal{L}\cup\mathcal{L}^{\text{new}}\cup\mathcal{L}^{\text{tie}},\forall t\in\mathcal{T},\forall k=1,...,n^{\text{LA}} \tag{9}$$

TABLE I
LOGIC OF EXISTING TIE-LINE CONNECTION STATUS

$o^{\text{line}}_{m,n,s,t}$	$z^{\text{har}}_{m,n,s}$	$z^{\text{on}}_{m,n,s,t}$	$u^{\text{line}}_{m,n,s,t}$
0	0	0	0
0	0	1	1
0	1	0	0
0	1	1	1
1	0	0	0
1	0	1	0
1	1	0	0
1	1	1	1

where, $\phi^k_{m,n}=\cos(2k\pi/n^{\text{LA}})$, $\chi^k_{m,n}=\sin(2k\pi/n^{\text{LA}})$, and $\psi^k_{m,n}=S_{m,n}\cdot\cos(\pi/n^{\text{LA}})$.

For existing regular lines, constraints (10a)-(10b) model the actual line connection status $u^{\text{line}}_{m,n,s,t}$ depending on the hazard status $o^{\text{line}}_{m,n,s,t}$ and hardening decision $z^{\text{har}}_{m,n,s}$. If a line is hardened, its status is assumed to be on, i.e., $u^{\text{line}}_{m,n,s,t}=1$ as indicated in (10a); otherwise, the line status is dependent on the hazard status $o^{\text{line}}_{m,n,s,t}$, i.e., $u^{\text{line}}_{m,n,s,t}=1-o^{\text{line}}_{m,n,s,t}$ as indicated in (10b). For lines that are not in the hardening candidate set, line statuses are directly modeled in (10c).

$$1\ge u^{\text{line}}_{m,n,s,t}\ge z^{\text{har}}_{m,n,s},\ \forall(m,n)\in\mathcal{L}\cap\mathcal{L}^{\text{har}}_s,\forall t\in\mathcal{T} \tag{10a}$$

$$1-o^{\text{line}}_{m,n,s,t}+z^{\text{har}}_{m,n,s}\ge u^{\text{line}}_{m,n,s,t}\ge 1-o^{\text{line}}_{m,n,s,t}, \quad \forall(m,n)\in\mathcal{L}\cap\mathcal{L}^{\text{har}}_s,\forall t\in\mathcal{T} \tag{10b}$$

$$u^{\text{line}}_{m,n,s,t}=1-o^{\text{line}}_{m,n,s,t},\ \forall(m,n)\in\mathcal{L}\backslash\mathcal{L}^{\text{har}}_s,\forall t\in\mathcal{T} \tag{10c}$$

For existing tie-lines, further considering the switching decisions complicate our modeling. The logic of tie-line connection status is shown in Table I. Note the hazard status $o^{\text{line}}_{m,n,s,t}$ can be 1 even when the switch of this tie-line is off. Equations (11a)-(11c) can exactly reflect the logic in Table I. If the switch status $z^{\text{on}}_{m,n,s,t}=1$, (11a)-(11c) is equivalent to (10a)-(10b); if $z^{\text{on}}_{m,n,s,t}=0$, we have $u^{\text{line}}_{m,n,s,t}=0$ from (11a) and (11c). For tie-lines that are not in the hardening candidate set, (11d)-(11e) can be simplified from (11a)-(11c).

$$z^{\text{on}}_{m,n,s,t}\ge u^{\text{line}}_{m,n,s,t}\ge z^{\text{har}}_{m,n,s}+z^{\text{on}}_{m,n,s,t}-1, \quad \forall(m,n)\in\mathcal{L}^{\text{tie}}\cap\mathcal{L}^{\text{har}}_s,\forall t\in\mathcal{T} \tag{11a}$$

$$1-o^{\text{line}}_{m,n,s,t}+z^{\text{har}}_{m,n,s}\ge u^{\text{line}}_{m,n,s,t}\ge z^{\text{on}}_{m,n,s,t}-o^{\text{line}}_{m,n,s,t}, \quad \forall(m,n)\in\mathcal{L}^{\text{tie}}\cap\mathcal{L}^{\text{har}}_s,\forall t\in\mathcal{T} \tag{11b}$$

$$u^{\text{line}}_{m,n,s,t}\ge 0,\ \forall(m,n)\in\mathcal{L}^{\text{tie}}\cap\mathcal{L}^{\text{har}}_s,\forall t\in\mathcal{T} \tag{11c}$$

$$z^{\text{on}}_{m,n,s,t}\ge u^{\text{line}}_{m,n,s,t}\ge 0,\ \forall(m,n)\in\mathcal{L}^{\text{tie}}\backslash\mathcal{L}^{\text{har}}_s,\forall t\in\mathcal{T} \tag{11d}$$

$$1-o^{\text{line}}_{m,n,s,t}\ge u^{\text{line}}_{m,n,s,t}\ge z^{\text{on}}_{m,n,s,t}-o^{\text{line}}_{m,n,s,t}, \quad \forall(m,n)\in\mathcal{L}^{\text{tie}}\backslash\mathcal{L}^{\text{har}}_s,\forall t\in\mathcal{T} \tag{11e}$$

For candidate regular lines, given the constraint of $z^{\text{har}}_{m,n,s}\le z^{\text{cons}}_{m,n}$ in (2d), the logic relations can be simplified, as shown in Table II. Again if the initial investment decision $z^{\text{cons}}_{m,n}=1$, (12a)-(12b) is equivalent to (10a)-(10b); if $z^{\text{cons}}_{m,n}=0$, we have $u^{\text{line}}_{m,n,s,t}=0$ from (12a) and (2d). Constraints (12c)-(12d) are for lines that are not in the hardening candidate set.

$$z^{\text{cons}}_{m,n}\ge u^{\text{line}}_{m,n,s,t}\ge z^{\text{har}}_{m,n,s},\ \forall(m,n)\in\mathcal{L}^{\text{new}}\cap\mathcal{L}^{\text{har}}_s,\forall t\in\mathcal{T} \tag{12a}$$

TABLE II
LOGIC OF CANDIDATE REGULAR LINE CONNECTION STATUS

$o^{\text{line}}_{m,n,s,t}$	$z^{\text{har}}_{m,n,s}$	$z^{\text{cons}}_{m,n}$	$u^{\text{line}}_{m,n,s,t}$
0	0	0	0
0	0	1	1
0	1	1	1
1	0	0	0
1	0	1	0
1	1	1	1

$$1-o^{\text{line}}_{m,n,s,t}+z^{\text{har}}_{m,n,s}\geq u^{\text{line}}_{m,n,s,t}\geq z^{\text{cons}}_{m,n}-o^{\text{line}}_{m,n,s,t},\quad \forall(m,n)\in\mathcal{L}^{\text{new}}\cap\mathcal{L}^{\text{har}}_s,\forall t\in\mathcal{T} \tag{12b}$$

$$z^{\text{cons}}_{m,n}\geq u^{\text{line}}_{m,n,s,t}\geq 0,\ \forall(m,n)\in\mathcal{L}^{\text{new}}\backslash\mathcal{L}^{\text{har}}_s,\forall t\in\mathcal{T} \tag{12c}$$

$$1-o^{\text{line}}_{m,n,s,t}\geq u^{\text{line}}_{m,n,s,t}\geq z^{\text{cons}}_{m,n}-o^{\text{line}}_{m,n,s,t},\quad \forall(m,n)\in\mathcal{L}^{\text{new}}\backslash\mathcal{L}^{\text{har}}_s,\forall t\in\mathcal{T} \tag{12d}$$

Note $u^{\text{line}}_{m,n,s,t}$ in (10)-(12) can be defined as continuous variables, however, values would be either 0 or 1.

5) Renewable Energy Constraints: We model the bounds for active power from existing and candidate renewable energy resources in (13a) and (13c), respectively, considering available generation capacities. Reactive power is assumed to be adjustable in (13b) and (13d). The $1-o^{\text{res}}_{i,s,t}$ terms in (13a)-(13b) and (13e) are used to ensure zero output when renewable energy resources encounter forced outages.

$$0\leq p_{i,s,t}\leq w^{\text{res}}_{i,s,t}\hat{p}^{\max}_i(1-o^{\text{res}}_{i,s,t}),\ \forall i\in\mathcal{W},\forall t\in\mathcal{T} \tag{13a}$$

$$-\hat{p}^{\max}_i(1-o^{\text{res}}_{i,s,t})\leq q_{i,s,t}\leq\hat{p}^{\max}_i(1-o^{\text{res}}_{i,s,t}),\quad \forall i\in\mathcal{W},\forall t\in\mathcal{T} \tag{13b}$$

$$0\leq p_{i,s,t}\leq w^{\text{res}}_{i,s,t}p^{\max}_i,\ \forall i\in\mathcal{W}^{\text{new}},\forall t\in\mathcal{T} \tag{13c}$$

$$-p^{\max}_i\leq q_{i,s,t}\leq p^{\max}_i,\ \forall i\in\mathcal{W}^{\text{new}},\forall t\in\mathcal{T} \tag{13d}$$

$$p_{i,s,t},q_{i,s,t}\leq\overline{P}^{\max}_i(1-o^{\text{res}}_{i,s,t}),\ q_{i,s,t}\geq-\overline{P}^{\max}_i(1-o^{\text{res}}_{i,s,t})\quad \forall i\in\mathcal{W}^{\text{new}},\forall t\in\mathcal{T} \tag{13e}$$

6) Mobile Storage Constraints: The operations of mobile energy storage units are modeled in (14). Variables for active charging and discharging power of mobile storage are bounded by the power capacity in (14a) and (14b), respectively. They are also subject to charging and discharging statuses, as shown in (14c) and (14d), respectively. Similarly, constraints for reactive power are presented in (14e) and (14f). The state of charge (SOC) in each time period is calculated in (14g). Equation (14h) defines the upper and lower bounds for SOC. The initial and end SOC values are defined in (14i) and (14j). The charging and discharging statuses of mobile storage can be non-zero only when it is connected to one of the buses, as modeled in (14k). For each time period, constraint (14l) guarantees a mobile storage unit is connected to at most one bus. The active and reactive injections from storage i to bus b are calculated in (14m) and (14n), respectively. Binary variables are declared in (14o)-(14p).

$$0\leq p^{\text{ch}}_{i,s,t}\leq p^{\max}_{i,s},\ \forall i\in\mathcal{E}^{\text{new}},\forall t\in\mathcal{T} \tag{14a}$$

$$0\leq p^{\text{dc}}_{i,s,t}\leq p^{\max}_{i,s},\ \forall i\in\mathcal{E}^{\text{new}},\forall t\in\mathcal{T} \tag{14b}$$

$$p^{\text{ch}}_{i,s,t}\leq\overline{P}^{\max}_i\beta^{\text{ch}}_{i,s,t},\ \forall i\in\mathcal{E}^{\text{new}},\forall t\in\mathcal{T} \tag{14c}$$

$$p^{\text{dc}}_{i,s,t}\leq\overline{P}^{\max}_i\beta^{\text{dc}}_{i,s,t},\ \forall i\in\mathcal{E}^{\text{new}},\forall t\in\mathcal{T} \tag{14d}$$

$$-p^{\max}_{i,s}\leq q_{i,s,t}\leq p^{\max}_{i,s},\ \forall i\in\mathcal{E}^{\text{new}},\forall t\in\mathcal{T} \tag{14e}$$

$$-\overline{P}^{\max}_i(\beta^{\text{ch}}_{i,s,t}+\beta^{\text{dc}}_{i,s,t})\leq q_{i,s,t}\leq\overline{P}^{\max}_i(\beta^{\text{ch}}_{i,s,t}+\beta^{\text{dc}}_{i,s,t}),\quad \forall i\in\mathcal{E}^{\text{new}},\forall t\in\mathcal{T} \tag{14f}$$

$$e_{i,s,t}=e_{i,s,t-1}+\eta^{\text{ch}}_i\cdot p^{\text{ch}}_{i,s,t}-\frac{1}{\eta^{\text{dc}}_i}\cdot p^{\text{dc}}_{i,s,t},\quad \forall i\in\mathcal{E}^{\text{new}},\forall t\in\mathcal{T} \tag{14g}$$

$$\underline{\gamma}_i e^{\max}_{i,s}\leq e_{i,s,t}\leq e^{\max}_{i,s},\ \forall i\in\mathcal{E}^{\text{new}},\forall t\in\mathcal{T}\backslash\{|\mathcal{T}|\} \tag{14h}$$

$$e_{i,s,0}=\gamma_{i,0}e^{\max}_{i,s},\ \forall i\in\mathcal{E}^{\text{new}} \tag{14i}$$

$$e_{i,s,|\mathcal{T}|}=\gamma_{i,0}e^{\max}_{i,s},\ \forall i\in\mathcal{E}^{\text{new}} \tag{14j}$$

$$\beta^{\text{ch}}_{i,s,t}+\beta^{\text{dc}}_{i,s,t}\leq\sum_{b\in\mathcal{B}^{\text{mes}}_i}\alpha_{i,b,s,t},\ \forall i\in\mathcal{E}^{\text{new}},\forall t\in\mathcal{T} \tag{14k}$$

$$\sum_{b\in\mathcal{B}^{\text{mes}}_i}\alpha_{i,b,s,t}\leq 1,\ \forall i\in\mathcal{E}^{\text{new}},\forall t\in\mathcal{T} \tag{14l}$$

$$p_{i,b,s,t}=\left(p^{\text{dc}}_{i,s,t}-p^{\text{ch}}_{i,s,t}\right)\alpha_{i,b,s,t},\quad \forall i\in\mathcal{E}^{\text{new}},\forall b\in\mathcal{B}^{\text{mes}}_i,\forall t\in\mathcal{T} \tag{14m}$$

$$q_{i,b,s,t}=q_{i,s,t}\alpha_{i,b,s,t},\ \forall i\in\mathcal{E}^{\text{new}},\forall b\in\mathcal{B}^{\text{mes}}_i,\forall t\in\mathcal{T} \tag{14n}$$

$$\alpha_{i,b,s,t}\in\{0,1\},\forall i\in\mathcal{E}^{\text{new}},\forall b\in\mathcal{B}^{\text{mes}}_i,\forall t\in\mathcal{T} \tag{14o}$$

$$\beta^{\text{ch}}_{i,s,t},\beta^{\text{dc}}_{i,s,t}\in\{0,1\},\ \forall i\in\mathcal{E}^{\text{new}},\forall t\in\mathcal{T} \tag{14p}$$

Note (14m) and (14n) are nonlinear constraints. Taking (14m) as an example, it is converted to equivalent mixed-integer linear constraints in (15).

$$-\overline{P}^{\max}_i\alpha_{i,b,s,t}\leq p_{i,b,s,t}\leq\overline{P}^{\max}_i\alpha_{i,b,s,t},\quad \forall i\in\mathcal{E}^{\text{new}},\forall b\in\mathcal{B}^{\text{mes}}_i,\forall t\in\mathcal{T} \tag{15a}$$

$$-\overline{P}^{\max}_i(1-\alpha_{i,b,s,t})+p^{\text{dc}}_{i,s,t}-p^{\text{ch}}_{i,s,t}\leq p_{i,b,s,t}\leq\overline{P}^{\max}_i(1-\alpha_{i,b,s,t})+p^{\text{dc}}_{i,s,t}-p^{\text{ch}}_{i,s,t},\quad \forall i\in\mathcal{E}^{\text{new}},\forall b\in\mathcal{B}^{\text{mes}}_i,\forall t\in\mathcal{T} \tag{15b}$$

7) Relaxed Formulation for Robust Modeling: We introduce a relaxation of $\vartheta_s(\boldsymbol{x},\boldsymbol{x}^{\text{adp}}_s,\boldsymbol{u}_s)$ in (4) to check the feasibility of operations under the worst case, which is modeled in (2a). The objective function in (16) is a penalty for infeasibility. Non-negative $\boldsymbol{\sigma}_s$ are defined as slack variables.

$$\tilde{\vartheta}_s(\boldsymbol{x},\boldsymbol{x}^{\text{adp}}_s,\boldsymbol{u}_s)=\min_{\boldsymbol{\sigma}_s\geq\mathbf{0},\boldsymbol{y}_s}\tilde{\text{M}}_\sigma\cdot(\mathbf{1}^\top\boldsymbol{\sigma}_s) \tag{16}$$

where, $\tilde{\text{M}}_\sigma$ is a big-M penalty factor.

8) Normal Scenario Formulation: The optimization problem in (4)-(7b), (7d), and (9)-(14) is formulated for extreme weather scenarios, however, it can be simplified for normal scenarios by letting the values of line hardening decision variables and mobile storage capacity variables be zeros.

D. Abstract Representation

The first-stage investment and second-stage re-investment problems are abstractly presented in (17a) and (17b), respectively. The third-stage operation problems for extreme weather and normal scenarios are presented in (17c) and (17e), respectively. The relaxed operation problem for feasibility checking is shown in (17d). The long-term uncertainties are described by scenarios s in a stochastic manner, which includes scenarios for multiple extreme weather events. Flexible adaptive re-investment modeling for extreme scenarios can

enable more affordable incorporation of multiple events that are traditionally considered unlikely to happen. The short-term uncertainties are described by event consequence realizations in uncertainty set $\mathcal{U}_s^{\text{xtm}}$ for extreme scenario s.

$$\min_{\boldsymbol{x}\in\mathcal{X}} \underbrace{\boldsymbol{c}^{\text{inv}\top}\boldsymbol{x}}_{\substack{\text{initial}\\ \text{investments}}} + \sum_{s\in\mathcal{S}^{\text{xtm}}} \Pr_s \cdot \varphi'_s(\boldsymbol{x}) + \sum_{s\in\mathcal{S}^{\text{nml}}} \Pr_s \cdot \vartheta'_s(\boldsymbol{x}) \tag{17a}$$

$$\varphi'_s(\boldsymbol{x}) = n^{\text{d}} \cdot \varphi_s(\boldsymbol{x}) = \min_{\boldsymbol{x}_s^{\text{adp}}\in\mathcal{X}_s^{\text{adp}}(\boldsymbol{x})} \Big(\underbrace{\boldsymbol{c}_s^{\text{adp}\top}\boldsymbol{x}_s^{\text{adp}}}_{\substack{\text{flexible}\\ \text{re-investments}}} + \vartheta'_s(\boldsymbol{x}, \boldsymbol{x}_s^{\text{adp}}, \hat{\boldsymbol{u}}_s) + \max_{\boldsymbol{u}_s\in\mathcal{U}_s^{\text{xtm}}} \tilde{\vartheta}'_s(\boldsymbol{x}, \boldsymbol{x}_s^{\text{adp}}, \boldsymbol{u}_s) \Big),\ \forall s \in \mathcal{S}^{\text{xtm}} \tag{17b}$$

$$\vartheta'_s(\boldsymbol{x}, \boldsymbol{x}_s^{\text{adp}}, \hat{\boldsymbol{u}}_s) = n^{\text{d}} \cdot \vartheta_s(\boldsymbol{x}, \boldsymbol{x}_s^{\text{adp}}, \hat{\boldsymbol{u}}_s) = \min_{\boldsymbol{y}_s\in\mathcal{Y}_s^{\text{xtm}}(\boldsymbol{x}, \boldsymbol{x}_s^{\text{adp}}, \hat{\boldsymbol{u}}_s)} \boldsymbol{c}_s^{\text{xtm}\top}\boldsymbol{y}_s,\ \forall s \in \mathcal{S}^{\text{xtm}} \tag{17c}$$

$$\tilde{\vartheta}'_s(\boldsymbol{x}, \boldsymbol{x}_s^{\text{adp}}, \hat{\boldsymbol{u}}_s) = n^{\text{d}} \cdot \tilde{\vartheta}_s(\boldsymbol{x}, \boldsymbol{x}_s^{\text{adp}}, \boldsymbol{u}_s) = \min_{(\boldsymbol{\sigma}_s, \tilde{\boldsymbol{y}}_s)\in\tilde{\mathcal{Y}}_s^{\text{xtm}}(\boldsymbol{x}, \boldsymbol{x}_s^{\text{adp}}, \boldsymbol{u}_s)} \text{M}_\sigma \cdot (\boldsymbol{1}^\top\boldsymbol{\sigma}_s),\ \forall s \in \mathcal{S}^{\text{xtm}} \tag{17d}$$

$$\vartheta'_s(\boldsymbol{x}) = n^{\text{d}} \cdot \vartheta_s(\boldsymbol{x}) = \min_{\boldsymbol{y}_s\in\mathcal{Y}_s^{\text{nml}}(\boldsymbol{x})} \boldsymbol{c}_s^{\text{nml}\top}\boldsymbol{y}_s,\ \forall s \in \mathcal{S}^{\text{nml}} \tag{17e}$$

where,

$$\mathcal{X} = \{\boldsymbol{x} : \boldsymbol{A}^{\text{inv}}\boldsymbol{x} \le \boldsymbol{b}^{\text{inv}}\} \tag{18a}$$

$$\mathcal{X}_s^{\text{adp}}(\boldsymbol{x}) = \{\boldsymbol{x}_s^{\text{adp}} : \boldsymbol{B}_s^{\text{adp}}\boldsymbol{x}_s^{\text{adp}} \le \boldsymbol{b}_s^{\text{adp}} - \boldsymbol{B}_s^{\text{inv}}\boldsymbol{x}\}, \quad \forall s \in \mathcal{S}^{\text{xtm}} \tag{18b}$$

$$\mathcal{Y}_s^{\text{xtm}}(\boldsymbol{x}, \boldsymbol{x}_s^{\text{adp}}, \hat{\boldsymbol{u}}_s) = \{\boldsymbol{y}_s^{\text{d}}, \boldsymbol{y}_s^{\text{c}} : \boldsymbol{C}_s^{\text{d}}\boldsymbol{y}_s^{\text{d}} + \boldsymbol{C}_s^{\text{c}}\boldsymbol{y}_s^{\text{c}} \le \boldsymbol{b}_s^{\text{xtm}} + \boldsymbol{C}_s^{\text{u}}\hat{\boldsymbol{u}}_s - \boldsymbol{C}_s^{\text{inv}}\boldsymbol{x} - \boldsymbol{C}_s^{\text{adp}}\boldsymbol{x}_s^{\text{adp}}\},\ \forall s \in \mathcal{S}^{\text{xtm}} \tag{18c}$$

$$\tilde{\mathcal{Y}}_s^{\text{xtm}}(\boldsymbol{x}, \boldsymbol{x}_s^{\text{adp}}, \boldsymbol{u}_s) = \{\boldsymbol{\sigma}_s, \boldsymbol{y}_s^{\text{d}}, \boldsymbol{y}_s^{\text{c}} : \boldsymbol{C}_s^{\text{d}}\boldsymbol{y}_s^{\text{d}} + \boldsymbol{C}_s^{\text{c}}\boldsymbol{y}_s^{\text{c}} \le \boldsymbol{b}_s^{\text{xtm}} + \boldsymbol{C}_s^{\text{u}}\boldsymbol{u}_s - \boldsymbol{C}_s^{\text{inv}}\boldsymbol{x} - \boldsymbol{C}_s^{\text{adp}}\boldsymbol{x}_s^{\text{adp}} + \boldsymbol{C}_s^{\sigma}\boldsymbol{\sigma}_s,\ \boldsymbol{\sigma}_s \ge \boldsymbol{0}\}, \quad \forall s \in \mathcal{S}^{\text{xtm}} \tag{18d}$$

$$\mathcal{Y}_s^{\text{nml}}(\boldsymbol{x}) = \{\boldsymbol{y}_s : \boldsymbol{D}_s\boldsymbol{y}_s \le \boldsymbol{b}_s^{\text{nml}} - \boldsymbol{D}_s^{\text{inv}}\boldsymbol{x}\},\ \forall s \in \mathcal{S}^{\text{nml}} \tag{18e}$$

$\mathcal{X}$ includes constraints in (1b)-(1c); $\mathcal{X}_s^{\text{adp}}(\boldsymbol{x})$ contains constraints in (2b)-(2f); $\mathcal{Y}_s^{\text{nml}}(\boldsymbol{x})$ and $\mathcal{Y}_s^{\text{xtm}}(\boldsymbol{x}, \boldsymbol{x}_s^{\text{adp}}, \hat{\boldsymbol{u}}_s)$ contains operation constraints in (5)-(7b), (7d), (9)-(14) that correspond to normal and extreme weather scenarios, respectively. $\tilde{\mathcal{Y}}_s^{\text{xtm}}(\boldsymbol{x}, \boldsymbol{x}_s^{\text{adp}}, \boldsymbol{u}_s)$ is a relaxation of $\mathcal{Y}_s^{\text{xtm}}(\boldsymbol{x}, \boldsymbol{x}_s^{\text{adp}}, \boldsymbol{u}_s)$. The cost terms for initial investments, re-investments, normal and emergent operations are denoted by $\boldsymbol{c}^{\text{inv}}$, $\boldsymbol{c}^{\text{adp}}$, $\boldsymbol{c}_s^{\text{nml}}$, and $\boldsymbol{c}_s^{\text{xtm}}$, respectively. M_σ is a big-M penalty factor. For the convenience of algorithmic description in section III-B, variables in $\boldsymbol{y}_s$ for extreme weather scenarios $s \in \mathcal{S}^{\text{xtm}}$ are separated to a discrete component in $\boldsymbol{y}_s^{\text{d}}$ and a continuous component in $\boldsymbol{y}_s^{\text{c}}$, as shown in (18c) and (18d). $\boldsymbol{c}^{\text{xtmd}}$ and $\boldsymbol{c}^{\text{xtmc}}$ represent the corresponding components of $\boldsymbol{c}^{\text{xtm}}$, thus $\boldsymbol{c}_s^{\text{xtm}\top}\boldsymbol{y}_s$ in (17c) is equivalent to $\boldsymbol{c}_s^{\text{xtmd}\top}\boldsymbol{y}_s^{\text{d}} + \boldsymbol{c}_s^{\text{xtmd}\top}\boldsymbol{y}_s^{\text{c}}$. Matrices $\boldsymbol{A}^{\cdot}$, $\boldsymbol{B}^{\cdot}$, $\boldsymbol{C}^{\cdot}$, $\boldsymbol{D}^{\cdot}$, and vectors $\boldsymbol{b}^{\cdot}$ are defined with different superscripts and/or subscripts for the purpose of abstract representation.

III. Solution Algorithm

A. Proposed Algorithm

We propose a novel PH algorithm that is embedded with a nested CCG method to solve (17). As the nested CCG procedure can iteratively identify worst-case short-term uncertainty realizations, it is used to check if current initial investment decisions can address the worst case in an outer loop. Meanwhile, the inner loop uses PH to solve (17) given previously identified short-term uncertainty realizations.

Our proposed algorithm is described in detail as follows.

Step 1: Outer Loop. Set outer iteration counter $J \leftarrow 1$.

Step 2: Inner Loop. Set inner iteration counter $K \leftarrow 1$ and multipliers $\boldsymbol{w}_s^{J,0} \leftarrow \boldsymbol{0}$, $\forall s \in \mathcal{S}$. Set termination threshold ϵ_{PH}.

Step 2-1: For each normal scenario $s \in \mathcal{S}^{\text{nml}}$, solve $\min_{\boldsymbol{x}\in\mathcal{X}, \boldsymbol{y}_s\in\mathcal{Y}_s^{\text{nml}}(\boldsymbol{x})} \boldsymbol{c}^{\text{inv}\top}\boldsymbol{x} + \boldsymbol{c}_s^{\text{nml}\top}\boldsymbol{y}_s$ and let $\hat{\boldsymbol{x}}_s^{J,K}$ denote optimal initial investments. For each extreme scenario $s \in \mathcal{S}^{\text{xtm}}$, get $\hat{\boldsymbol{x}}_s^{J,K}$ by solving (19). As described later in Step 4, $\mathcal{J}_{s,J}$ is the set of indices for uncertainty realizations identified by the nested CCG algorithm in the J-th outer iteration.

$$\begin{aligned} \min\quad & \boldsymbol{c}^{\text{inv}\top}\boldsymbol{x} + \boldsymbol{c}_s^{\text{adp}\top}\boldsymbol{x}_s^{\text{adp}} + \boldsymbol{c}_s^{\text{xtm}\top}\boldsymbol{y}_s \\ \text{s.t.}\quad & \boldsymbol{x} \in \mathcal{X},\ \boldsymbol{x}_s^{\text{adp}} \in \mathcal{X}_s^{\text{adp}}(\boldsymbol{x}), \\ & \boldsymbol{y}_s \in \mathcal{Y}_s^{\text{xtm}}(\boldsymbol{x}, \boldsymbol{x}_s^{\text{adp}}, \hat{\boldsymbol{u}}_s), \\ & \boldsymbol{y}_s^{(j,m)} \in \mathcal{Y}_s^{\text{xtm}}(\boldsymbol{x}, \boldsymbol{x}_s^{\text{adp}}, \hat{\boldsymbol{u}}_s^{(j,m)}), \\ & \qquad \forall (j,m) \in \cup_{j'=1,\ldots,J-1}\mathcal{J}_{s,j'} \end{aligned} \tag{19}$$

Step 2-2: Aggregate the first-stage solutions with $\bar{\boldsymbol{x}}^{J,K} = \sum_{s\in\mathcal{S}} \Pr_s \cdot \hat{\boldsymbol{x}}_s^{J,K}$. Update multipliers with $\boldsymbol{w}_s^{J,K}(i) = \boldsymbol{w}_s^{J,K-1}(i) + \nu^K \boldsymbol{\rho}(i)(\hat{\boldsymbol{x}}_s^{J,K}(i) - \bar{\boldsymbol{x}}^{J,K}(i)), \forall i \in \mathcal{I}_x, \forall s \in \mathcal{S}$. Here $\mathcal{I}_x$ is the set of indices for first-stage investment variables; $\boldsymbol{\rho}$ are parameters defined later in (22); ν^K is an acceleration factor; and (i) represents the i-th entry of a vector. If $\sum_{s\in\mathcal{S}} \Pr_s \cdot \left\| \hat{\boldsymbol{x}}_s^{J,K} - \bar{\boldsymbol{x}}^{J,K} \right\| \le \epsilon_{\text{PH}}$, where $\|\cdot\|$ represents 2-norm, denote the obtained first-stage solution by $\hat{\boldsymbol{x}}^J \leftarrow \bar{\boldsymbol{x}}^{J,K}$, go to Step 3; otherwise, go to Step 2-3.

Step 2-3: Update inner iteration counter $K \leftarrow K + 1$. For each normal scenario $s \in \mathcal{S}^{\text{nml}}$, solve optimization problem $\min_{\boldsymbol{x}\in\mathcal{X}, \boldsymbol{y}_s\in\mathcal{Y}_s^{\text{nml}}(\boldsymbol{x})} \boldsymbol{c}^{\text{inv}\top}\boldsymbol{x} + \boldsymbol{c}_s^{\text{nml}\top}\boldsymbol{y}_s + \boldsymbol{w}_s^{J,K-1\top}\boldsymbol{x} + \sum_{i\in\mathcal{I}_x} \frac{\boldsymbol{\rho}(i)}{2} \left\| \boldsymbol{x}(i) - \bar{\boldsymbol{x}}^{J,K-1}(i) \right\|^2$ and let $\hat{\boldsymbol{x}}_s^{J,K}$ denote optimal initial investments. For each extreme scenario $s \in \mathcal{S}^{\text{xtm}}$, calculate $\hat{\boldsymbol{x}}_s^{J,K}$ by solving (20). Go to Step 2-2.

$$\begin{aligned} \min\quad & \boldsymbol{c}^{\text{inv}\top}\boldsymbol{x} + \boldsymbol{c}_s^{\text{adp}\top}\boldsymbol{x}_s^{\text{adp}} + \boldsymbol{c}_s^{\text{xtm}\top}\boldsymbol{y}_s + \boldsymbol{w}_s^{J,K-1\top}\boldsymbol{x} \\ & + \sum\nolimits_{i\in\mathcal{I}_x} \frac{\boldsymbol{\rho}(i)}{2} \left\| \boldsymbol{x}(i) - \bar{\boldsymbol{x}}^{J,K-1}(i) \right\|^2 \\ \text{s.t.}\quad & \boldsymbol{x} \in \mathcal{X},\ \boldsymbol{x}_s^{\text{adp}} \in \mathcal{X}_s^{\text{adp}}(\boldsymbol{x}), \\ & \boldsymbol{y}_s \in \mathcal{Y}_s^{\text{xtm}}(\boldsymbol{x}, \boldsymbol{x}_s^{\text{adp}}, \hat{\boldsymbol{u}}_s), \\ & \boldsymbol{y}_s^{(j,m)} \in \mathcal{Y}_s^{\text{xtm}}(\boldsymbol{x}, \boldsymbol{x}_s^{\text{adp}}, \hat{\boldsymbol{u}}_s^{(j,m)}), \\ & \qquad \forall (j,m) \in \cup_{j'=1,\ldots,J-1}\mathcal{J}_{s,j'} \end{aligned} \tag{20}$$

Step 3: Use nested CCG algorithm, as shown in Steps C1-C7 in section III-B, to solve (21) for all $s \in \mathcal{S}^{\text{xtm}}$ with updated

values of $\hat{\boldsymbol{x}}^J$ from Step 2.

$$\min_{\substack{\boldsymbol{x}_s^{\mathrm{adp}}\in\mathcal{X}_s^{\mathrm{adp}}(\hat{\boldsymbol{x}}^J),\ \boldsymbol{y}_s\in\mathcal{Y}_s^{\mathrm{xtm}}(\hat{\boldsymbol{x}}^J,\boldsymbol{x}_s^{\mathrm{adp}},\hat{\boldsymbol{u}}_s),\ \boldsymbol{y}_s^{(j,m)}\in \\ \mathcal{Y}_s^{\mathrm{xtm}}(\boldsymbol{x},\boldsymbol{x}_s^{\mathrm{adp}},\hat{\boldsymbol{u}}_s^{(j,m)})\ \forall(j,m)\in\cup_{j'=1,\dots,J-1}\mathcal{J}_{s,j'}}} \big(\boldsymbol{c}_s^{\mathrm{adp}\top}\boldsymbol{x}_s^{\mathrm{adp}}+ \boldsymbol{c}_s^{\mathrm{xtm}\top}\boldsymbol{y}_s+\max_{\boldsymbol{u}_s\in\mathcal{U}_s^{\mathrm{xtm}}}\min_{(\boldsymbol{\sigma}_s,\tilde{\boldsymbol{y}}_s)\in\tilde{\mathcal{Y}}_s^{\mathrm{xtm}}(\hat{\boldsymbol{x}}^J,\boldsymbol{x}_s^{\mathrm{adp}},\boldsymbol{u}_s)} \mathrm{M}_\sigma\cdot(\mathbf{1}^\top\boldsymbol{\sigma}_s)\big) \tag{21}$$

Step 4: Denote the set of indices for new uncertainty realizations founded in Step 3 by $\mathcal{J}_{s,J}$. If $\mathcal{J}_{s,J}=\varnothing$ for all $s\in\mathcal{S}^{\mathrm{xtm}}$, terminate and output the obtained solution; otherwise, add feasibility cuts $\boldsymbol{y}_s^{(j,m)}\in\mathcal{Y}_s^{\mathrm{xtm}}(\boldsymbol{x},\boldsymbol{x}_s^{\mathrm{adp}},\hat{\boldsymbol{u}}_s^{(j,m)}),\ \forall(j,m)\in\mathcal{J}_{s,J}$ to (19) and (20), update outer iteration counter $J\leftarrow J+1$, and go to Step 2.

Note although the PH algorithm has been widely adopted to solve mixed-integer programs in the literature, its convergence is not theoretically guaranteed in general [21]. To improve the converging performance, element-specific values for $\boldsymbol{\rho}$ are used in Steps 2-2 and 2-3. $\boldsymbol{\rho}$ can be chosen cost-proportionally [21], as shown in (22), wherein k_ρ is a constant factor.

$$\boldsymbol{\rho}(i)=k_\rho\cdot\boldsymbol{c}^{\mathrm{inv}}(i),\ \forall i\in\mathcal{I}_x \tag{22}$$

B. Implementation of Nested CCG Algorithm

An improved nested CCG algorithm [22], [26] is used in Step 3 of the proposed algorithm, as binary variables appearing in emergent operation problems result in a mixed-integer third stage for $s\in\mathcal{S}^{\mathrm{xtm}}$. We elaborate on the steps of the improved nested CCG algorithm here. The details are available in [26].
Step C1: Define termination thresholds $\varepsilon_{\mathrm{outer}}$ and $\varepsilon_{\mathrm{inner}}$ for outer and inner loops of nested CCG algorithm, respectively. Initialize for the outer CCG loop: set outer counter $M\leftarrow 1$, and bounds $u_{\mathrm{outer}}\leftarrow+\infty$, $l_{\mathrm{outer}}\leftarrow-\infty$. Initialize set of indices $\mathcal{J}_{s,J}\leftarrow\varnothing$ for future identified uncertainty realizations.
Step C2: Solve the optimization problem in (23). Optimality cuts are modeled for $(j,m)\in\mathcal{J}_{s,J}$ to avoid infeasibility. Denote the optimal solution of adaptive planning decisions, base-case discrete and continuous emergent operation decisions by $\hat{\boldsymbol{x}}_s^{\mathrm{adp}(J,M)}$, $\hat{\boldsymbol{y}}_s^{\mathrm{d}(J,M)}$ and $\hat{\boldsymbol{y}}_s^{\mathrm{c}(J,M)}$, respectively. Let $\hat{\kappa}_s^{(J,M)}=\boldsymbol{c}_s^{\mathrm{adp}\top}\hat{\boldsymbol{x}}_s^{\mathrm{adp}(J,M)}+\boldsymbol{c}_s^{\mathrm{xtmd}\top}\hat{\boldsymbol{y}}_s^{\mathrm{d}(J,M)}+\boldsymbol{c}_s^{\mathrm{xtmc}\top}\hat{\boldsymbol{y}}_s^{\mathrm{c}(J,M)}$. Updated the optimal objective value to l_{outer}.

$$\begin{aligned}
&\min_{\substack{\boldsymbol{x}_s^{\mathrm{adp}},\boldsymbol{y}_s^{\mathrm{d}},\boldsymbol{y}_s^{\mathrm{c}},\boldsymbol{\sigma}_s^{(j,m)},\\ \boldsymbol{y}_s^{\mathrm{d}(j,m)},\boldsymbol{y}_s^{\mathrm{c}(j,m)},\varrho}} \boldsymbol{c}_s^{\mathrm{adp}\top}\boldsymbol{x}_s^{\mathrm{adp}}+\boldsymbol{c}_s^{\mathrm{xtmd}\top}\boldsymbol{y}_s^{\mathrm{d}}+\boldsymbol{c}_s^{\mathrm{xtmc}\top}\boldsymbol{y}_s^{\mathrm{c}}+\varrho\\
&\text{s.t. } \boldsymbol{B}_s^{\mathrm{adp}}\boldsymbol{x}_s^{\mathrm{adp}}\le\boldsymbol{b}_s^{\mathrm{adp}}-\boldsymbol{B}_s^{\mathrm{inv}}\hat{\boldsymbol{x}}^J,\\
&\boldsymbol{C}_s^{\mathrm{adp}}\boldsymbol{x}_s^{\mathrm{adp}}+\boldsymbol{C}_s^{\mathrm{d}}\boldsymbol{y}_s^{\mathrm{d}}+\boldsymbol{C}_s^{\mathrm{c}}\boldsymbol{y}_s^{\mathrm{c}}\le\boldsymbol{b}_s^{\mathrm{xtm}}+\boldsymbol{C}_s^{\mathrm{u}}\hat{\boldsymbol{u}}_s-\boldsymbol{C}_s^{\mathrm{inv}}\hat{\boldsymbol{x}}^J,\\
&\boldsymbol{C}_s^{\mathrm{adp}}\boldsymbol{x}_s^{\mathrm{adp}}+\boldsymbol{C}_s^{\mathrm{d}}\boldsymbol{y}_s^{\mathrm{d}(j,m)}+\boldsymbol{C}_s^{\mathrm{c}}\boldsymbol{y}_s^{\mathrm{c}(j,m)}\le\boldsymbol{b}_s^{\mathrm{xtm}}+\boldsymbol{C}_s^{\mathrm{u}}\hat{\boldsymbol{u}}_s^{(j,m)}\\
&\qquad-\boldsymbol{C}_s^{\mathrm{inv}}\hat{\boldsymbol{x}}^J,\ \forall(j,m)\in\cup_{j'=1,\dots,J-1}\mathcal{J}_{s,j'}\\
&\boldsymbol{C}_s^{\mathrm{adp}}\boldsymbol{x}_s^{\mathrm{adp}}+\boldsymbol{C}_s^{\mathrm{d}}\boldsymbol{y}_s^{\mathrm{d}(j,m)}+\boldsymbol{C}_s^{\mathrm{c}}\boldsymbol{y}_s^{\mathrm{c}(j,m)}-\boldsymbol{C}_s^{\sigma}\boldsymbol{\sigma}_s^{(j,m)}\le\boldsymbol{b}_s^{\mathrm{xtm}}\\
&\qquad+\boldsymbol{C}_s^{\mathrm{u}}\hat{\boldsymbol{u}}_s^{(j,m)}-\boldsymbol{C}_s^{\mathrm{inv}}\hat{\boldsymbol{x}}^J,\ \forall(j,m)\in\mathcal{J}_{s,J}\\
&\mathrm{M}_\sigma\cdot\left(\mathbf{1}^\top\boldsymbol{\sigma}_s^{(j,m)}\right)\le\varrho,\ \mathbf{0}\le\boldsymbol{\sigma}_s^{(j,m)},\ \forall(j,m)\in\mathcal{J}_{s,J}
\end{aligned}\tag{23}$$

Step C3: Initialize for the inner CCG loop: set inner counter $N\leftarrow 1$, and bounds $u_{\mathrm{inner}}\leftarrow+\infty$, $l_{\mathrm{inner}}\leftarrow-\infty$.
Step C4: Solve the problem in (24). Noticing variables in $\boldsymbol{u}_s^{(N)}$ are binary, the nonlinear term $\left(\boldsymbol{C}_s^{\mathrm{u}}\boldsymbol{u}_s\right)^\top\boldsymbol{\lambda}_s^{(n)}$ in (25) can be linearized with the technique used in (15). More details are available in [27]. Therefore, (24) can be equivalently converted to a mixed-integer linear program. In contrast to the heuristic approach used in [26], the method to solve (24) in this work is exact. Update the optimal objective value to u_{inner}. Denote the optimal solution of uncertainty realization by $\hat{\boldsymbol{u}}_s^{(N)}$. For $N=1$, $\hat{\boldsymbol{u}}_s^{(1)}$ can be given by an initial guess.

$$\begin{aligned}
&\hat{\kappa}_s^{(J,M)}+\max_{\eta,\boldsymbol{u}_s}\eta\\
&\text{s.t. }\ \eta\le\varsigma_s\left(\hat{\boldsymbol{x}}_s^{\mathrm{adp}(J,M)},\hat{\boldsymbol{y}}_s^{\mathrm{d}(n)},\boldsymbol{u}_s\right),\ \forall n=1,\dots,N-1\\
&\qquad\boldsymbol{u}_s\in\mathcal{U}_s^{\mathrm{xtm}}
\end{aligned}\tag{24}$$

where,

$$\begin{aligned}
\varsigma_s\left(\hat{\boldsymbol{x}}_s^{\mathrm{adp}(J,M)},\ \hat{\boldsymbol{y}}_s^{\mathrm{d}(n)},\boldsymbol{u}_s\right)=\max_{\boldsymbol{\lambda}_s^{(n)}}&\Big[\boldsymbol{b}_s^{\mathrm{xtm}}+\boldsymbol{C}_s^{\mathrm{u}}\boldsymbol{u}_s-\boldsymbol{C}_s^{\mathrm{inv}}\hat{\boldsymbol{x}}^J\\
&-\boldsymbol{C}_s^{\mathrm{adp}}\hat{\boldsymbol{x}}_s^{\mathrm{adp}(J,M)}-\boldsymbol{C}_s^{\mathrm{d}}\hat{\boldsymbol{y}}_s^{\mathrm{d}(n)}\Big]^\top\boldsymbol{\lambda}_s^{(n)}\\
\text{s.t. }\ &\boldsymbol{C}_s^{\mathrm{c}\top}\boldsymbol{\lambda}_s^{(n)}=\mathbf{0},\\
&-\boldsymbol{C}_s^{\sigma\top}\boldsymbol{\lambda}_s^{(n)}\le\mathrm{M}_\sigma\cdot\mathbf{1},\\
&\boldsymbol{\lambda}_s^{(n)}\le\mathbf{0}
\end{aligned}\tag{25}$$

Step C5: Solve the optimization problem in (26). Let $\hat{\boldsymbol{y}}_s^{\mathrm{d}(N)}$ denote the optimal solution of discrete operation variables. Update the optimal objective value to l_{inner}.

$$\begin{aligned}
&\hat{\kappa}_s^{(J,M)}+\min_{\boldsymbol{\sigma}_s^{(N)}\ge0,\boldsymbol{y}_s^{\mathrm{d}(N)},\boldsymbol{y}_s^{\mathrm{c}(N)}}\mathrm{M}_\sigma\cdot\left(\mathbf{1}^\top\boldsymbol{\sigma}_s^{(N)}\right)\\
&\text{s.t. }\boldsymbol{C}_s^{\mathrm{d}}\boldsymbol{y}_s^{\mathrm{d}(N)}+\boldsymbol{C}_s^{\mathrm{c}}\boldsymbol{y}_s^{\mathrm{c}(N)}-\boldsymbol{C}_s^{\sigma}\boldsymbol{\sigma}_s^{(N)}\le\\
&\qquad\boldsymbol{b}_s^{\mathrm{xtm}}+\boldsymbol{C}_s^{\mathrm{u}}\hat{\boldsymbol{u}}_s^{(N)}-\boldsymbol{C}_s^{\mathrm{inv}}\hat{\boldsymbol{x}}^J-\boldsymbol{C}_s^{\mathrm{adp}}\hat{\boldsymbol{x}}_s^{\mathrm{adp}(J,M)}
\end{aligned}\tag{26}$$

Step C6: Check if the inner CCG loop converges with criteria $u_{\mathrm{inner}}-l_{\mathrm{inner}}\le\varepsilon_{\mathrm{inner}}$. If not, $N\leftarrow N+1$, and go to Step C4; otherwise, update u_{outer} with the optimal solution from the inner CCG loop, let $\hat{\boldsymbol{u}}_s^{(J,M)}\leftarrow\hat{\boldsymbol{u}}_s^{(N)}$, and go to Step C7.
Step C7: Check if the CCG outer loop converges by examining $u_{\mathrm{outer}}-l_{\mathrm{outer}}\le\varepsilon_{\mathrm{outer}}$. If not, update $\mathcal{J}_{s,J}\leftarrow\mathcal{J}_{s,J}\cup\{(J,M)\}$, $M\leftarrow M+1$, and go to Step C2; otherwise, terminate.

IV. Case Study

We tested our proposed approach by using 33-bus and 141-bus test systems. All the mixed-integer linear program (MILP) and mixed-integer quadratic program (MIQP) problems were solved by CPLEX 12.10 [28]. Part of our mathematical models were built with YALMIP [29].

A. Modified IEEE 33-Bus Test System

The tested IEEE 33-bus system in this work is a modified version of the case presented in [24]. For the purpose of planning a distribution system with renewables, we add existing wind power sources at buses 3, 6, and 10, candidate wind power sources at buses 2, 22, and 25, as well as several candidate lines. Besides scenarios that represent normal operation conditions, three hazard scenarios that reflect the uncertainties of extreme weather event consequences are considered in

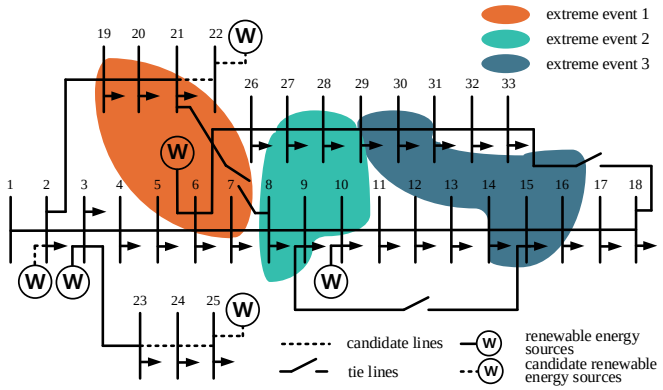

Fig. 3. Modified IEEE 33-bus system diagram and affected areas in extreme weather events.

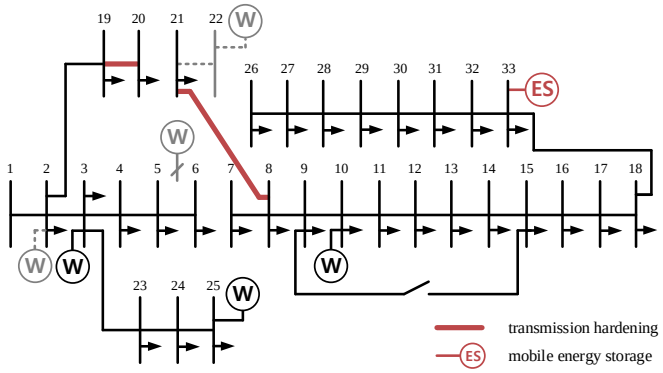

Fig. 4. A snapshot of operations for extreme scenario 1 in modified IEEE 33-bus system.

our case study. These scenarios also reveal the patterns of demands, wind power outputs, and LMPs at the root node. As shown in Fig. 3, relatively diverse spatial distributions of outages for multiple extreme weather events may bring challenges for cost-effective and resilient planning.

1) Planning Results and Extreme Event Response: By using our proposed multi-stage adaptive approach, the planning results for modified 33-bus distribution system are listed in Table III. We use three cases for comparison: in case 1, adaptive planning options for both line hardening and mobile energy renting are allowed after early warnings of extreme weather events are received; while in case 2 and case 3, only one of these options is considered to be adaptive. In our test cases, the number of hardened distribution lines is constrained up to two considering the time and crew limits. As shown in Table III, in comparison to cases 2 and 3, the advantage of our adaptive planning approach in case 1 is that initial investment decisions are less conservative, because adaptive planning decision-making against each extreme weather event can be performed after early warnings are received.

The proposed resilience-oriented planning approach also considers the flexibility of tie-line switching for extreme weather events. Given initial and adaptive investment decisions, a snapshot of emergent operations for extreme scenario 1 is illustrated in Fig. 4. As indicated, the coordination of mobile storage scheduling, line hardening, and tie-line switching enables re-connections to power sources for most feeders that suffer from extreme weather events. This shows adaptive re-investment decisions can effectively enhance preparedness for resilient operations under extreme weather events.

2) Benefit from Adaptive Planning of Distribution Line Hardening: We further analyze the benefit from the proposed adaptive planning approach with a detailed comparison of case 1 and case 2 in Table III. Case 2 is designed with non-adaptive distribution line hardening. The line hardening decisions are made in the first stage as *here-and-now* variables in case 2. As line hardening works are not required to implement under relatively limited time and crew conditions, the constraints in (2e) can be relaxed. In addition, the hardening also yields a lower cost in a non-emergent case. In our numeral simulations in Table III, we assume the cost of adaptive hardening in case 1 is 20% more than that of non-adaptive hardening considered in the first stage of case 2. As shown in the planning results of case 2, the non-adaptive hardening is made for 7 lines, which aims to cover diverse consequences of extreme weather events. Considering the low probabilities of these events, making hardening decisions for all the possibilities can be expensive. This is verified in the investment and overall cost comparisons

TABLE III
PLANNING RESULT COMPARISONS FOR MODIFIED IEEE 33-BUS SYSTEM

cases	initial investments	adaptive re-investments			annualized cost (10^3\$)		
		extreme scenario 1	extreme scenario 2	extreme scenario 3	investments	operations	total
case 1 (adaptive planning)	line 23-24, line 24-25, WPS* with 0.8 MW at bus 25	hardening line 19-20, line 21-8, renting MES* with 2.2 MW, 24.0 MWh	hardening line 27-28, line 9-15, renting MES with 1.7 MW, 13.1 MWh	hardening line 15-16, line 9-15, renting MES with 0.4 MW, 2.9 MWh	1493.0	455.3	1948.3
case 2 (non-adaptive hardening, adaptive mobile storage)	line 23-24, line 24-25, WPS with 0.8 MW at bus 25, hardening line 15-16, line 19-20, line 27-28, line 28-29, line 21-8, line 9-15, line 18-33	renting MES with 2.2 MW, 24.0 MWh	renting MES with 0.4 MW, 0.07 MWh	-	1924.5	455.3	2379.9**
case 3 (adaptive hardening, non-adaptive mobile storage)	line 23-24, line 24-25, WPS with 0.8 MW at bus 25, MES with 2.2 MW, 24.0 MWh	hardening line 19-20, and line 21-8	hardening line 28-29, and line 9-15	hardening line 15-16, and line 18-33	2616.4	347.4	2963.8

* WPS and MES are the abbreviations of "wind power sources" and "mobile energy storage", respectively.
** The inconsistency of investment plus operation cost and total cost on the first digit after the decimal point is caused by rounding error.

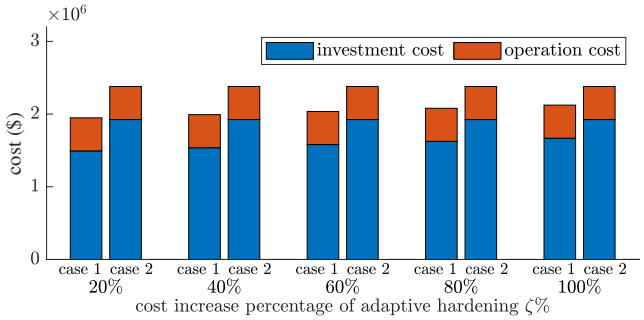

Fig. 5. Sensitivity to cost increase percentage of adaptive hardening.

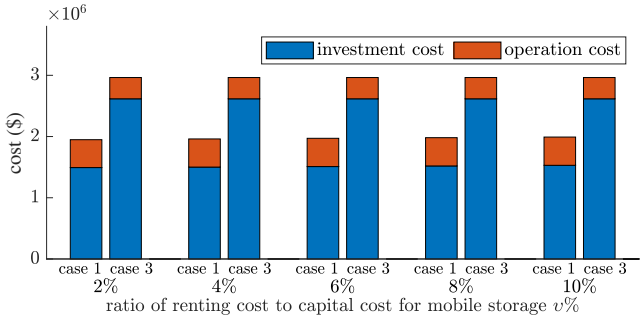

Fig. 6. Sensitivity to the ratio of renting cost to capital cost for mobile storage.

of case 1 and case 2.

The cost increase percentage of adaptive hardening on the basis of non-adaptive hardening could be important for the total system cost of planning decisions from the proposed approach. By defining the cost increase percentage as $\zeta\%$, we have $c^{\text{har}}_{m,n,s} = (1+\zeta\%)\cdot c^{\text{har}}_{m,n}$, where $c^{\text{har}}_{m,n,s}$ and $c^{\text{har}}_{m,n}$ are costs for adaptive and non-adaptive hardening of line (m,n), respectively. The sensitivity of the cost-effectiveness comparison between case 1 and case 2 to this cost rise is shown in Fig. 5. As indicated, the total cost for the adaptive approach slightly increases as the defined cost increase percentage $\zeta\%$ increases. Meanwhile, the cost benefit from our adaptive hardening model still exists even in the 100% case, as the non-adaptive hardening approach over-conservatively hardens lines for all the low-probability extreme weather events.

3) Benefit from Adaptive Planning of Mobile Storage: Another comparison is between the proposed adaptive approach and an approach with non-adaptive planning decisions of mobile storage, i.e. case 1 and case 3 in Table III. In case 3, mobile storage decisions are made in the first stage, while line hardening decisions are allowed to be adjustable in the second stage for extreme weather events. The cost of renting mobile energy storage for a few days is assumed to be less than the capital cost. In our numerical experiment, both the per-MW and per-MWh renting costs are assumed to be 2% of corresponding capital costs. On the other hand, owning rather than renting mobile energy storage facilities can benefit the normal operation of distribution systems. As shown in Table III, purchasing mobile storage would result in higher investment costs. Meanwhile, the total operation cost is reduced as the arbitrage capability of mobile storage can be utilized in normal operations. As the capital cost of

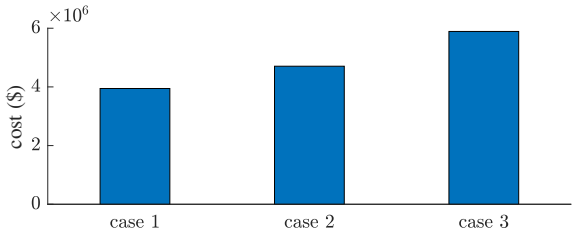

Fig. 7. Cost comparison in modified 141-bus system.

battery storage is expensive, we observe the operation cost reduction through daily arbitrage cannot cover the investment cost difference between purchasing and renting mobile storage in our test case. Therefore, the total cost of case 1 is less than that of case 3 in Table III.

A sensitivity analysis of the total system cost to the ratio of renting cost to capital cost $\upsilon\%$ is also conducted. As shown in Fig. 6, the renting cost has a weak impact on the total cost, because it is a small portion of the total investment cost. Therefore, if the renting cost to capital cost ratio $\upsilon\%$ is in a reasonable range, the proposed planning approach can offer more flexible and cost-effective investment decisions in comparison to the approach in case 3. Note although purchasing mobile storage is not shown to be cost-effective in our simulation, it could be useful in other circumstances. Our formulation can be easily extended to include mobile storage investment decisions in the first stage.

B. Modified 141-Bus Test System

A modified 141-bus system, which is originally presented in [30] with typos corrected in [31], is also used in our case study. To test our approach in distribution system planning, candidate lines, tie-lines, existing and candidate renewable energy resources are added. The diagram for this system is shown in [27]. We also incorporate three extreme weather scenarios in this test. As designed similarly to the previous IEEE 33-bus system: case 1 implements our proposed approach, which allows adaptive planning for both line hardening and mobile energy renting; case 2 models non-adaptive hardening but adaptive mobile storage; and case 3 considers adaptive hardening but non-adaptive mobile storage. As shown in Fig. 7, the proposed approach presented by case 1 also yields a lower cost, in comparison to two other cases. This reflects the adaptive planning approach can reduce the total cost by enabling planning flexibility.

V. Conclusion

We present a resilience-oriented multi-stage adaptive planning model for distribution systems in this work. A novel PH algorithm embedded with a nested CCG procedure is used to solve our model. The main conclusions of this paper are:

1) Our approach has benefits in making flexible planning decisions to reduce investment and total system costs when multiple low-probability extreme weather events are simultaneously considered. Flexible re-investments are shown to be more cost-effective compared to making all the decisions in the initial investments.

2) The proposed CCG-embedded PH algorithm can successfully solve challenging multi-stage hybrid-stochastic-and-robust problems in our numerical simulation. The algorithm is tested in both modified IEEE 33-bus and 141-bus systems.

The formulation in this work can be further extended to consider stationary energy storage and tie-line investments.

REFERENCES

[1] NBC News. Texas sees power outages in heat wave for the ages. [Online]. Available: https://www.nbcnews.com/id/wbna44019419

[2] J. Mark. A Texas meteorologist warned of power outages. Then the lights went out. [Online]. Available: https://www.washingtonpost.com/nation/2022/07/15/texas-meteorologist-lights-heat-wave/

[3] KHOU. Power outage tracker: Clusters of outages remain in Galveston, Lake Jackson and Houston. [Online]. Available: https://www.khou.com/article/weather/severe-weather/centerpoint-power-outages-tropical-storm-nicholas/285-b4106ad1-3604-4503-982f-7246bcda1c06

[4] C. King, J. Rhodes, J. Zarnikau *et al.* The timeline and events of the February 2021 Texas electric grid blackouts. [Online]. Available: https://energy.utexas.edu/ercot-blackout-2021

[5] N. S. Ray-Bennett, "Multiple disasters and policy responses in pre-and post-independence Orissa, India," *Disasters*, vol. 33, no. 2, pp. 274–290, 2009.

[6] The Guardian. Interactive map: which areas of Australia were hit by multiple disasters in 2020? [Online]. Available: https://www.theguardian.com/news/datablog/2020/dec/22/interactive-map-which-areas-of-australia-were-hit-by-multiple-disasters-in-2020

[7] Q. P. Zheng, J. Wang, P. M. Pardalos, and Y. Guan, "A decomposition approach to the two-stage stochastic unit commitment problem," *Ann. Oper. Res.*, vol. 210, no. 1, pp. 387–410, 2013.

[8] B. Hu and L. Wu, "Robust SCUC considering continuous/discrete uncertainties and quick-start units: A two-stage robust optimization with mixed-integer recourse," *IEEE Trans. Power Syst.*, vol. 31, no. 2, pp. 1407–1419, 2015.

[9] S. Wang, C. Zhao, L. Fan, and R. Bo, "Distributionally robust unit commitment with flexible generation resources considering renewable energy uncertainty," *IEEE Trans. Power Syst.*, vol. 37, no. 6, pp. 4179–4190, 2022.

[10] D. Mejía-Giraldo and J. D. McCalley, "Maximizing future flexibility in electric generation portfolios," *IEEE Trans. Power Syst.*, vol. 29, no. 1, pp. 279–288, 2013.

[11] S. Lei, C. Chen, H. Zhou, and Y. Hou, "Routing and scheduling of mobile power sources for distribution system resilience enhancement," *IEEE Trans. on Smart Grid*, vol. 10, no. 5, pp. 5650–5662, 2018.

[12] S. Lei, C. Chen, Y. Li, and Y. Hou, "Resilient disaster recovery logistics of distribution systems: Co-optimize service restoration with repair crew and mobile power source dispatch," *IEEE Trans. on Smart Grid*, vol. 10, no. 6, pp. 6187–6202, 2019.

[13] Q. Zhang, Z. Wang, S. Ma, and A. Arif, "Stochastic pre-event preparation for enhancing resilience of distribution systems," *Renewable Sustain. Energy Rev.*, vol. 152, p. 111636, 2021.

[14] J. Kim and Y. Dvorkin, "Enhancing distribution system resilience with mobile energy storage and microgrids," *IEEE Trans. on Smart Grid*, vol. 10, no. 5, pp. 4996–5006, 2018.

[15] S. Ma, B. Chen, and Z. Wang, "Resilience enhancement strategy for distribution systems under extreme weather events," *IEEE Trans. on Smart Grid*, vol. 9, no. 2, pp. 1442–1451, 2016.

[16] S. Ma, L. Su, Z. Wang, F. Qiu, and G. Guo, "Resilience enhancement of distribution grids against extreme weather events," *IEEE Trans. Power Syst.*, vol. 33, no. 5, pp. 4842–4853, 2018.

[17] Y. Lin and Z. Bie, "Tri-level optimal hardening plan for a resilient distribution system considering reconfiguration and DG islanding," *Appl. Energy*, vol. 210, pp. 1266–1279, 2018.

[18] G. Zhang, F. Zhang, X. Zhang, Q. Wu, and K. Meng, "A multi-disaster-scenario distributionally robust planning model for enhancing the resilience of distribution systems," *Int. J. Electr. Power Energy Syst.*, vol. 122, p. 106161, 2020.

[19] A. Shahbazi, J. Aghaei, S. Pirouzi, M. Shafie-khah, and J. P. Catalão, "Hybrid stochastic/robust optimization model for resilient architecture of distribution networks against extreme weather conditions," *Int. J. Electr. Power Energy Syst.*, vol. 126, p. 106576, 2021.

[20] R. T. Rockafellar and R. J.-B. Wets, "Scenarios and policy aggregation in optimization under uncertainty," *Math. Oper. Res.*, vol. 16, no. 1, pp. 119–147, 1991.

[21] J.-P. Watson and D. L. Woodruff, "Progressive hedging innovations for a class of stochastic mixed-integer resource allocation problems," *Comput. Manag. Sci.*, vol. 8, no. 4, pp. 355–370, 2011.

[22] L. Zhao and B. Zeng. (2012) An exact algorithm for two-stage robust optimization with mixed integer recourse problems. [Online]. Available: http://www.optimization-online.org/DB_FILE/2012/01/3310.pdf

[23] 7th AIMMS–MOPTA optimization modeling competition. [Online]. Available: https://coral.ise.lehigh.edu/~mopta2015/AIMMS_MOPTA_case_2015.pdf

[24] M. E. Baran and F. F. Wu, "Network reconfiguration in distribution systems for loss reduction and load balancing," *IEEE Trans. Power Deliv.*, vol. 4, no. 2, pp. 1401–1407, 1989.

[25] Z. Tan, H. Zhong, Q. Xia, C. Kang, X. S. Wang, and H. Tang, "Estimating the robust PQ capability of a technical virtual power plant under uncertainties," *IEEE Trans. Power Syst.*, vol. 35, no. 6, pp. 4285–4296, 2020.

[26] S. Wang, G. Geng, and Q. Jiang, "Robust co-planning of energy storage and transmission line with mixed integer recourse," *IEEE Trans. Power Syst.*, vol. 34, no. 6, pp. 4728–4738, 2019.

[27] S. Wang and R. Bo. Supplementary material for "A resilience-oriented multi-stage adaptive distribution system planning considering multiple extreme weather events". [Online]. Available: https://github.com/ee-swang/supplementary-material/blob/main/SUPPL-TSTE-00225-2022.pdf

[28] IBM. ILOG CPLEX Homepage. [Online]. Available: https://www.ibm.com/products/ilog-cplex-optimization-studio/cplex-optimizer

[29] J. Löfberg. YALMIP. [Online]. Available: https://yalmip.github.io/

[30] H. Khodr, F. Olsina, P. De Oliveira-De Jesus, and J. Yusta, "Maximum savings approach for location and sizing of capacitors in distribution systems," *Electr. Power Syst. Res.*, vol. 78, no. 7, pp. 1192–1203, 2008.

[31] R. D. Zimmerman, C. E. Murillo-Sánchez, and R. J. Thomas, "Matpower: Steady-state operations, planning, and analysis tools for power systems research and education," *IEEE Trans. Power Syst.*, vol. 26, no. 1, pp. 12–19, 2011.

Siyuan Wang (Member, IEEE) received the B.S. and Ph.D. degrees both in electrical engineering from Zhejiang University, Hangzhou, China. He is currently a Postdoctoral Fellow at Johns Hopkins University, Baltimore, USA. His research interests include power system operation and planning, renewable energy integration, and applications of energy storage technology in power systems.

Rui Bo (Senior Member, IEEE) received the BSEE and MSEE degrees in electric power engineering from Southeast University (China) in 2000 and 2003, respectively, and received the Ph.D. degree in electrical engineering from the University of Tennessee, Knoxville (UTK) in 2009. He is currently an Assistant Professor of the Electrical and Computer Engineering Department at the Missouri University of Science and Technology (formerly University of Missouri-Rolla). He worked as a Principal Engineer and Project Manager at Midcontinent Independent System Operator (MISO) from 2009 to 2017. His research interests include computation, optimization, and economics in power system operation and planning, high-performance computing, electricity market simulation, evaluation, and design.